6-1-1970

An Optical Technique for On-Film Recording of Lens Aperture and Focus Settings

Richard Thompson

AN OPTICAL TECHNIQUE FOR ON-FILM RECORDING OF LENS APERTURE AND FOCUS SETTINGS

by

Richard E. Thompson
NASA - Manned Spacecraft Center

This thesis is submitted in partial fulfillment of the requirements for a Master of Science degree in Photographic Science at the Rochester Institute of Technology.

June, 1970

Thesis adviser: John F. Carson

Approved:

Thesis Adviser _____

_____

_____

_____

ACKNOWLEDGEMENTS

I am very pleased to acknowledge the continual support and guidance provided by Professors John Carson and Albert Rickmers of the Rochester Institute of Technology. In addition, I wish to thank those who contributed information and equipment for this research: Jeff Bremer and the Photographic Technology Laboratory, NASA - MSC; Östen Wejerfelt, Victor Hasselblad AB; Dr. Hans Sauer, Carl Zeiss; and Jerry Kovanda, Paillard Inc. Special mention must be made of the valuable assistance with computer techniques provided by Joel Gray.

TABLE OF CONTENTS

LIST OF TABLES

LIST OF FIGURES

AN OPTICAL TECHNIQUE FOR ON-FILM RECORDING OF LENS APERTURE AND FOCUS SETTINGS

by

Richard E. Thompson
NASA - Manned Spacecraft Center

An Abstract

This thesis is submitted in partial fulfillment of the requirements for a Master of Science degree in Photographic Science at the Rochester Institute of Technology.

June, 1970

Thesis adviser: John F. Carson

ABSTRACT

A simple optical technique for placing a record of the camera aperture and focus conditions on each photograph is described. A lens system is installed in a NASA/Hasselblad lunar surface camera so that a small image of the camera iris is formed in the corner of the photographic image field. The camera aperture and focus settings that were used in the taking of the photograph are determined from measurements of the width and position of the data image. A Fortran IV computer program which uses the system calibration data and iterative techniques to determine the settings from the image measurements is used and described.

The relatively simple system employed in this investigation was able to resolve camera aperture settings of half-stop increments in the range of f/5.6 to f/16. In addition to detecting the three calibrated focus settings of 5, 15, and 70 feet, the focus values of 3, 3.5, 4, and 8 feet also could be distinguished. Since the camera iris opening is imaged, a measure of the inherent iris variability is obtained during normal system calibration.

I. INTRODUCTION

I. INTRODUCTION

The photographs returned from the Apollo lunar missions are of intense immediate interest to the public, but the true measure of their worth will be gauged by the quantitative data that can be extracted from them. The Hasselblad still cameras used by the astronauts during their lunar surface activities are specially designed to enhance data retrieval without sacrificing camera flexibility and ease of operation.[1] Photogrammetric and photometric evaluation of the lunar landing and exploration areas are made possible with these cameras. However, this evaluation is hampered presently by the lack of a record of which camera lens aperture and focus settings were used to obtain each photograph. The astronauts certainly cannot be expected to make such a record during their already demanding surface activities, nor to remember which settings were used for any of the several hundred photographs obtained while on the lunar surface.

Since lunar surface reflectance has a very strong dependence upon the azimuth and elevation of the sun, relative slopes and elevations of the surface can be determined through photometric comparisons in and among the returned photographs.[2] To utilize accurately this technique, the photometric transfer characteristics of the camera itself must be known. The pre-flight camera calibrations provide the required illuminance distribution in the film plane as a function of the lens aperture and focus settings. Since the settings now used range from f/5.6 to f/11 for aperture, and from 3 feet to infinity for focus, a considerable range of illuminance distributions exists. Only by knowing what settings were used can the

proper camera illuminance distribution be applied to the photometric data of the photograph.

Probably the most important use of the lunar surface photographs comes in their photogrammetric applications. The measurement of objects of interest and the general reconstruction of the area topography are possible with this terrestrial photogrammetry.[3-4] The variability of focus, however, presents problems not usually encountered in photogrammetric situations. As the focus setting is changed, the principal distance or camera constant changes accordingly, affecting both distortion and scaling. In order to obtain some calibration points in the focus range, detented click-stops are provided at four focus settings, and the photographic operations plans and crew training emphasize their use. Better confidence could be placed on the derived metric data, however, if a positive record of the camera focus condition existed.

From this brief discussion, it is clear that a record of the aperture and focus settings would assist greatly in the evaluation of lunar surface photographs. This thesis investigates the practicability of determining the lens aperture and focus settings by measuring the width and position of an image of the camera lens iris opening. A small optical system is installed in a NASA/Hasselblad lunar surface camera in such a way as to place an image of the camera lens iris in a corner of the picture area. By selecting an off-axis location for the image, a minimum amount of useful picture area is lost and the detection of focusing changes is made possible.

The axial location of the iris changes with camera focusing. From the off-axis position of the data lens, the movement of the iris corresponds to both a distance and an angular change. The angular variation results in lateral movement of the data image and the distance change causes a slight alteration of the size and focus of the image. The size of the data image is determined primarily by the size of the camera iris opening which is related directly to the aperture setting.

This thesis investigation, therefore, is to answer the following questions:

(1) Can the optical data system record the lens aperture settings in the range of f/5.6 to f/16 with half-stop resolution?

(2) Can the optical data system record the lens focus so that the detented settings of 5, 15, and 70 feet are distinguishable?

These performance goals are slightly more stringent than required by the current lunar surface photographic operations which specify exposure changes in full-stop increments in the range from f/5.6 to f/11 and which emphasize these detented focus settings. Since the lens aperture ring has detented click-stops every half-stop, it is realistic to seek this finer aperture resolution so that the unintentional, but highly probable, mid-stop settings may be detected. The focus record resolution would permit the photogrammetrist to select the appropriate calibration data for each photograph with greater confidence.

II. THEORETICAL DESIGN

II. THEORETICAL DESIGN

The theoretical concepts of this data system are merely those which are basic to any rotationally symmetric optical imaging device: the system image is proportional in size and in position to that of the object, the camera lens iris. The iris size changes with aperture setting and the iris position changes with focus setting. The task then becomes one of engineering design related to a specific camera. The optical design of the data system for the Hasselblad camera in question was performed in accordnace with accepted design techniques and is described in the following subsections.[5-7]

A. First-Order Considerations

The Hasselblad EL Data Camera with its Zeiss 60mm, f/5.6, Biogon lens is shown diagrammatically in Figure 1a and is documented by the engineering drawings of references 8 through 10. The lens is bayonet mounted to the front of the camera body to permit easy removal, and the rear structure of the lens extends into the body nearly 42mm. A glass plate is positioned immediately in front of the camera film plane. This plate is attached rigidly to the camera body and has fine reseau crosses engraved on its outer surface. These crosses serve as the fixed references to which the photometric and photogrammetric calibrations of the camera are referred. In addition, the glass reseau plate has a raised glass rim down each vertical side of its rear surface to keep the film from actually touching the image area of the plate. Since the film is pressed against the glass rims by the mechanism of the film magazine, the rims determine the actual film plane for the camera.

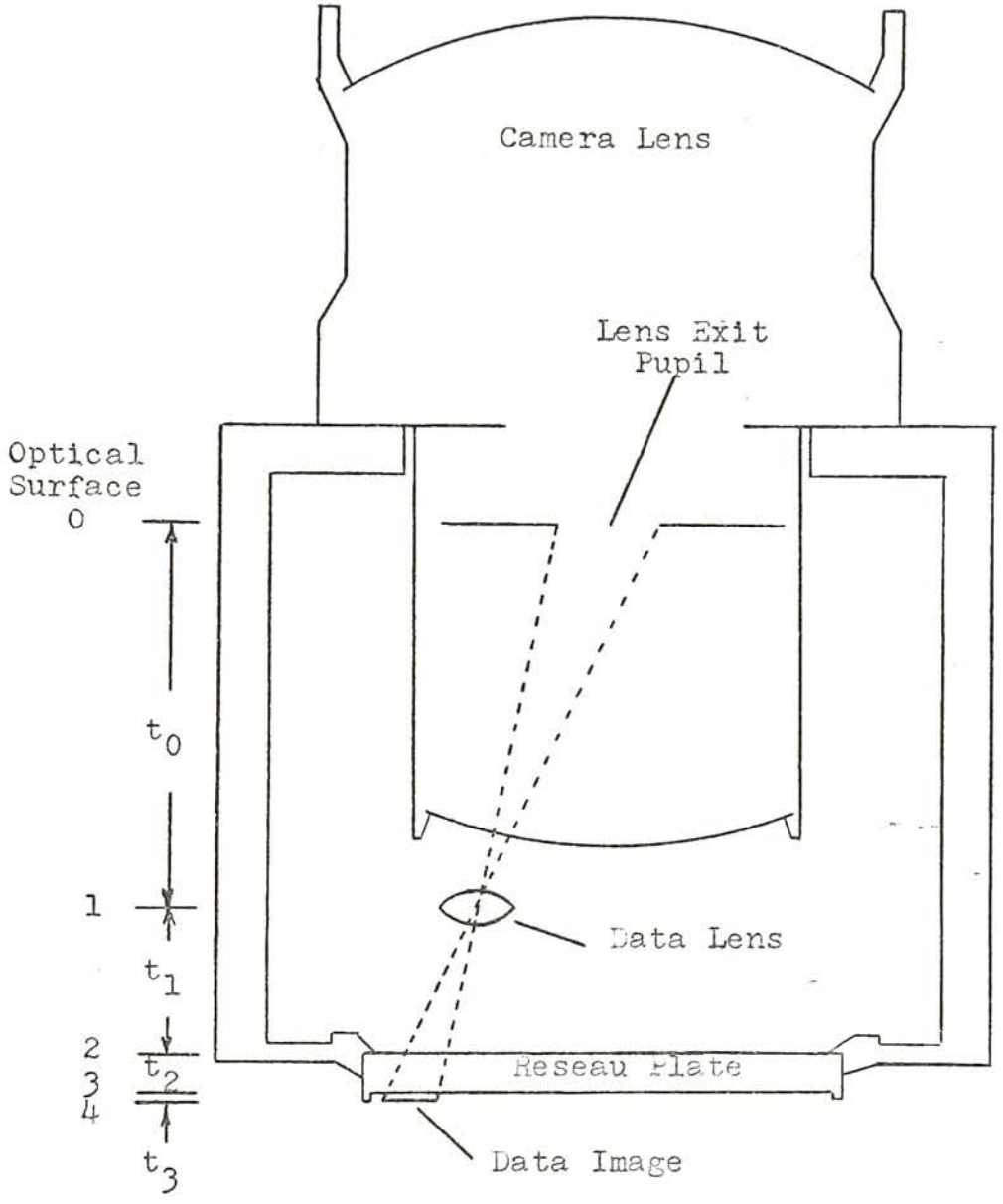

$(t_0 + t_1)$ = 57.39mm at infinity focus; 61.82mm at 3 feet focus
t_2 = 4.00mm t_3 = 0.10mm

(Drawing not to scale)

Figure 1a. Optical layout of lunar surface camera and proposed data system.

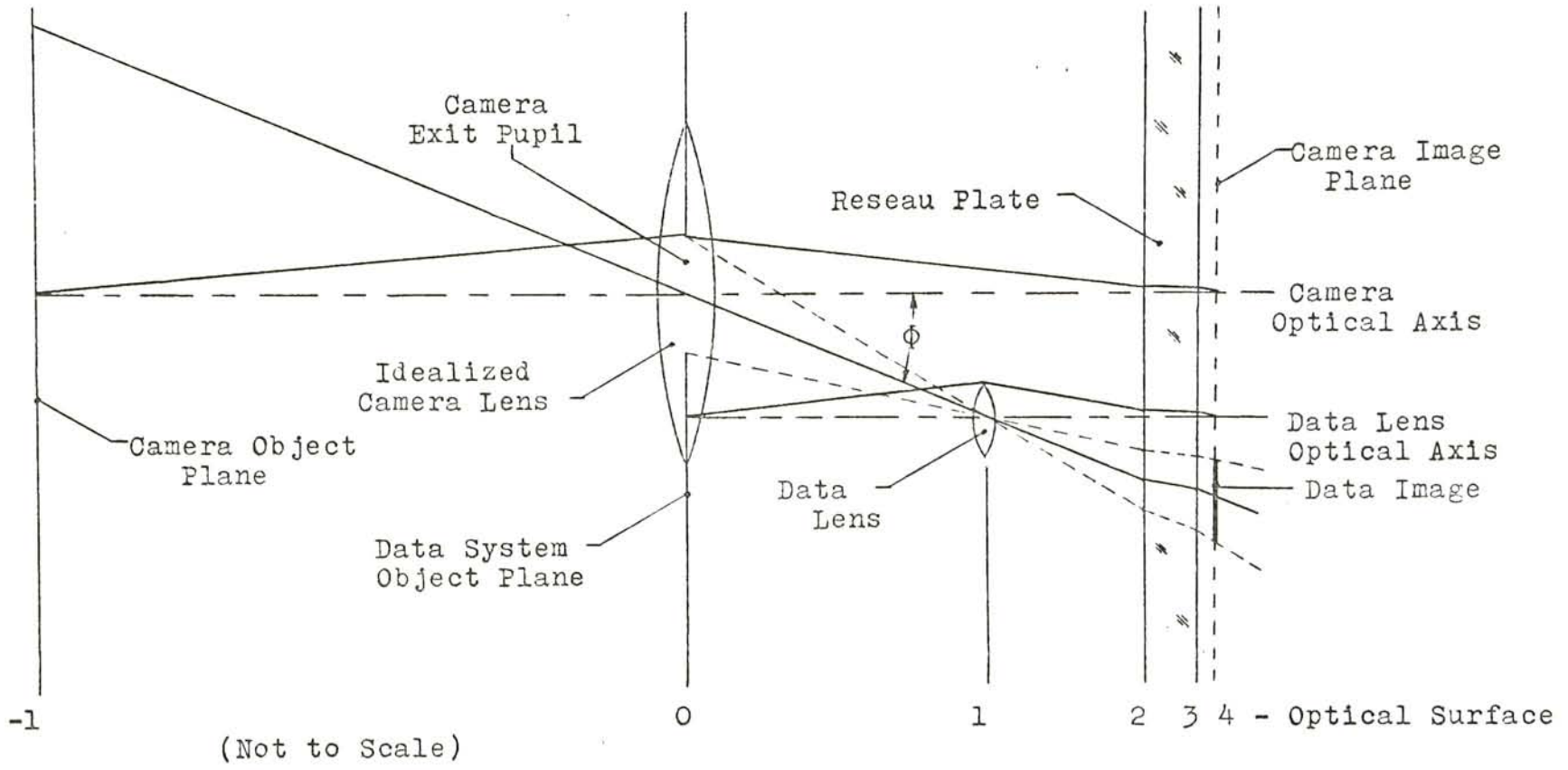

Figure 1b. Optical diagram of object and image relationships.

The optical surfaces that must be considered in the design of the data system are indicated at the left of the camera in Figure 1a and are shown diagrammatically in Figure 1b. The zeroth surface represents the lens exit pupil which is the iris image as viewed from the camera film plane with the reseau plate removed. By using the lens exit pupil data supplied by Carl Zeiss,[11] the optical effects of the rear elements of the lens can be neglected for first order considerations. The data lens, surface one, is assumed to be optically thin for the initial calculations. Surfaces two and three represent the boundaries of the glass reseau plate and surface four is the camera film plane.

For paraxial approximations, the required data lens focal length, f_1, is given by

$$f_1 = \frac{t_0 \, (t_1 + t_{2/n_2} + t_3)}{t_0 + t_1 + t_{2/n_2} + t_3}$$

where n_2 is the refractive index of the reseau plate and t_0, t_1, t_2, and t_3 are the distances between the optical surfaces as shown in Figures 1a and 1b. The data image can be in exact focus for only one position of the camera lens because of the dependence of f_1 on t_0. Since the primary interest in focus data is at the 5 feet detented setting, the data lens should be optimized for this camera focus. The design dimensions and numerical values for the data lens focal length and associated parameters covered in the following optical considerations are presented in detail in Appendix A.

Upper limits are placed on the data lens focal length from both optical and physical considerations. When the data lens focal length is increased from a small value, the data lens itself must be moved toward the camera exit pupil in order to keep the image focused at the film plane. The maximum focal length that will satisfy the focus condition is equal to one-fourth the optical distance between the exit pupil and the film. This value is 15.7mm for a camera focus setting of five feet. However, the physical extension of the camera lens into the camera body limits the distance the data lens can be moved toward the pupil. This physical limitation restricts the maximum data lens focal length to 15mm.

The magnification of the data system is

$$M_1 = - \frac{f_1}{t_0 - f_1}$$

and is dependent upon the camera focus setting through t_0. This dependence produces the required lateral motion of the data image as the camera focus is changed. Since the position and size changes of the image increase with the magnification, a large value is desirable; the magnification for a 12mm focal length ranges between -.33 and -.38 and between -.61 and -.74 for a 15mm focal length. A magnification large enough to provide the required data resolution is necessary, while too large a value will produce an undesirably large data image, thereby using too much of the picture area.

The effective aperture of the data lens must be selected to provide a usable data image illuminance. Since

the camera exit pupil is the object for the data lens, the data image illuminance will be proportional to the luminance of the camera pupil. For a diffuse scene and a well-corrected camera lens, the exit pupil luminance, B_0, is related directly to the scene luminance, B_s, as

$$B_o = \tau_o B_s$$

where τ_o is the camera lens transmission factor. The data image illuminance, E_1, is provided by

$$E_1 = \frac{\pi \tau_1 B_o \cos^4 \phi}{4 (f/)_1^2 (|M_1| + 1)^2}$$

where τ_1 is the data lens transmission, Φ is the off-axis angle, M_1 is the data lens magnification, and $(f/)_1$ is the aperture ratio of the data lens. Since the scene luminance can vary throughout a considerable range, the data lens aperture must be a compromise value. The photographic illuminance, E_0, at the center of the frame is related to the pupil luminance by

$$E_o = \frac{\pi B_o}{4 (f/)_o^2}$$

where $(f/)_0$ is the aperture setting for the camera lens. If the data image illuminance is set equal to the photographic illuminance, the data lens aperture ratio can be written

$$(f/)_1 = \frac{\sqrt{\tau_1}\,(f/)_o \cos^2 \phi}{(|M_1| + 1)}$$

and the data lens aperture diameter, D_1, is then

$$D_1 = \frac{f_1(|M_1| + 1)}{\sqrt{\tau_1}(f/)_o \cos^2\phi}$$

The proper compromise for the data lens aperture is obtained by selecting $(f/)_o$ as the average of the camera aperture values used in the operational situation.

Table 1 summarizes the parameter ranges, indicated by the preceeding discussion and the detailed coverage in Appendix A, for a data system that images in the picture area between a corner reseau cross and the frame corner.

Table 1. Thin-lens parameter ranges for a corner imaging data system

Parameter	Range
Focal Length	12 to 14 mm
Distance to Reseau Plate	13.4 to 18.4 mm
Lateral Location	25 to 21 mm
Off-Axis Angle	29° to 27°
Aperture Diameter	1.8 to 2.5 mm

When the data lens is considered to have thickness, surface number one becomes two surfaces and the inter-surface distances must be compensated so that the total exit pupil to reseau plate distance remains constant.

B. Third-Order Considerations

In order to achieve a more realistic assessment of the data system optical characteristics, it was necessary to consider the third-order aberration contributions. The required computations for this analysis were performed on a Royal McBee, LGP-30, electronic computer, available in the Institute's School of Photographic Arts and Sciences. The primary goal of this third-order investigation was to determine if a single element data lens possibly could be used to satisfy the system requirements. A data lens of almost any desired complexity and correction could be produced commercially, but the time and funding available for this research demanded simplicity.

The single element goal meant that no optical correction of the chromatic aberrations would be possible. Since the longitudinal and lateral chromatic aberrations would affect image size and position respectively, good color correction was highly desirable. Spectral filtering for the data system was considered, but this approach would have complicated image exposure and would have increased spherical aberration as the data lens aperture was increased to compensate for the loss in light transmission.

Since the data image was to be considerably off-axis, coma could become very large and cause the data image to be highly smeared. Fortunately, coma always can be removed by the appropriate placement of the lens stop. However, the camera places physical limits on how far away the stop can be from the data lens, and the farther away, the greater the chance of vignetting in the data lens assembly.

An equally detrimental off-axis aberration was that of astigmatism because it would result in unequal focus of the sagittal and tangential edges of the data image. Since all four of these edges could be used in the measurements of the image, it was very desirable that they be equally sharp. Associated with astigmatism is the basic Petzval curvature of the image field. However, this aberration was of only minor importance in the data system considerations because the data image would reside in only a small zone of the field. It would be quite simple to compensate for this curvature by shifting the data lens axially until the curved zone intersected the camera film plane.

Spherical aberration always must be considered, but in the case of the data system it was less important than color, coma, or astigmatism correction.[12] The best way to control the spherical aberration of this single element system was to keep the data lens aperture as small as possible.

The least important aberration of all was distortion because its effects would be included in the system calibration and would be repeatably reproduced in this small zone of interest.

For a single element data lens, the variations in stop position and in surface curvatures were the primary means of correcting the aberrations. Since this provided just three degrees of freedom, only a compromise correction of the third-order aberrations was possible. The resultant aberration coefficients were determined as functions of the three parameters, and graphical presentations as shown in Appendix A were used to select the best compromise optical design. When the additional constraint

of good lens availability was included in the determination, the best single element design became that of a plano-convex lens with the stop located a short distance from the plane surface which faced the camera lens. Table 2 summarizes the resulting system design parameters for a 12mm focal length data lens.

Table 2. Design parameters for a 12mm focal length data system

	Parameter	Design Value
a.	Stop aperture diameter	2mm
b.	Distance from stop to plane surface of data lens	2.3mm
c.	Front surface curvature	$0.000mm^{-1}$
d.	Data lens thickness	2.5mm
e.	Rear surface curvature	$-0.161mm^{-1}$
f.	Distance from rear surface to reseau plate	11.5mm

It is interesting to note that while the design shown in Table 2 placed the sagittal astigmatic focus of the data image on the film, the first-order axial focus was more than 1.8mm behind the camera film plane because of the field curvature effects. The process of shifting the data lens assembly to correct for field curvature was not as straightforward as first imagined. For example, as the data lens was moved to correct a focus error at the film plane, the data lens to camera iris distance also changed in such a way as to cancel some of the expected focus shift. This focusing characteristic actually is quite beneficial because it permits larger data lens to image movements and thereby makes

actual lens installation less critical.

The imaging properties of the optical design were evaluated by using ray intercept curves and spot diagrams as shown in Appendix A. The ray intercept curves provided a convenient representation of the effects of astigmatic focus differences and of chromatic and spherical aberrations. The spot diagram furnished similar information, but in a more physically interpretable form. By scanning the spot diagram, it was possible to predict edge sharpness and to calculate the modulation transfer characteristics of the data system.[6] These techniques indicated that the image position variation due to chromatic aberration would be less than 13% of the total position shift from a camera focus change of 5 feet to infinity. Furthermore, the sagittal edges of the data image would be spread only 10 micrometers and those in the tangential direction, only about 25 micrometers. The modulation transfer function for a radial scan of the spot diagram predicted a decrease to 10% modulation at a spatial frequency of 45 cycles per millimeter. These image quality estimates, though rather low for usual photographic use, indicated that the plano-convex design exhibited sufficient merit and could be tried in the camera.

III. EXPERIMENTAL PROCEDURE

III. EXPERIMENTAL PROCEDURE

Following the completion of the theoretical design, actual testing of a data system incorporated into a Hasselblad lunar surface camera was performed as described in the following subsections.

A. Data System Assembly

The data lens assembly is shown in an exploded view in Figure 2. The primary constructional material used in the assembly was telescoping brass tubing obtained at a hobby supply store in outside diameters of 11/32, 5/16, and 9/32 inch. The plano-convex lens with 15mm focal length and 9mm diameter was mounted on a short section of the 5/16 inch tubing with epoxy cement. The aperture stop was made by soldering a piece of .012 inch thick brass shim to the end of a section of the 9/32 inch tubing and then by drilling a 3/32 inch hole in the shim at the center of the tube. The rough edges of the metal surfaces were removed until the stop tube could be slipped freely inside the lens tube.

The mounting support for the lens-stop subassembly also was made from the tubing. A piece of the 9/32 inch tubing was soldered to a very short section of the 11/32 inch tubing so that the lens-stop assembly could be slipped into the 11/32 inch tube. A short section of the 5/16 inch tubing was soldered to a 1 by 3/4 inch piece of the shim material at a 45° angle. The 9/32 inch tubing of the support arm could then be inserted into the angled tubing of the mounting plate to complete the data lens assembly.

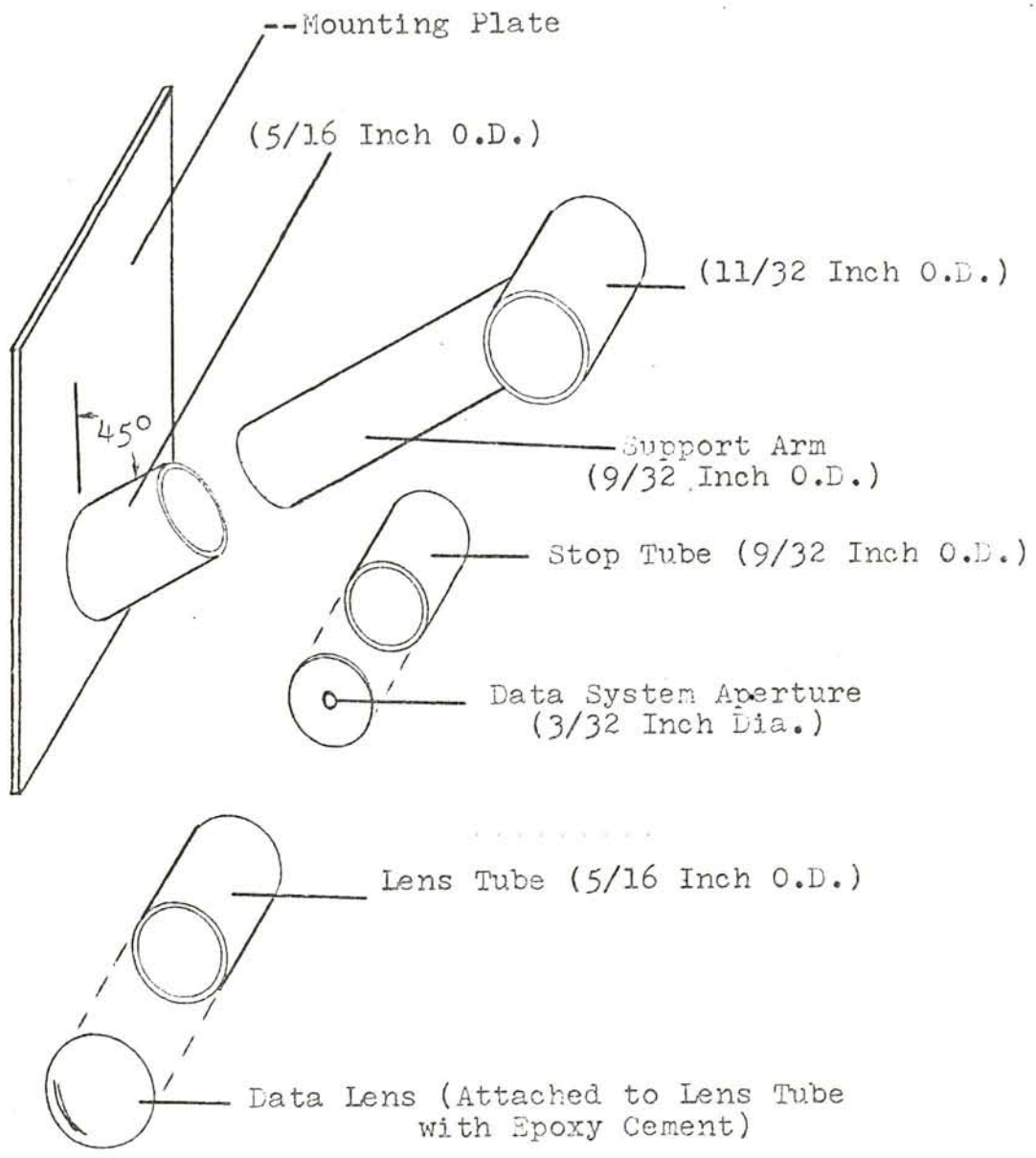

Figure 2. Exploded view of data lens assembly.

This constructional technique offered many advantages during system assembly into the camera. The data lens was to be installed in such a way that its image would be positioned on the lower left diagonal of the camera image between the outer reseau cross and the frame corner. This alignment was obtained in several steps. First, the bottom edge of the mounting plate was removed until the axis of the angled tubing was aligned with the frame diagonal when the mounting plate was flat against the left inside wall and touching the inside floor of the camera. The support arm was then shortened until the data image was correctly positioned when the arm was inserted into the angle tubing of the mount. Gross focus adjustment of the image was obtained by axial movement of the entire data assembly and fine adjustment was obtained by sliding the lens tube in the large tube of the support arm. The shadow cast on the camera image plane by the data assembly was reduced along the diagonal by grinding the outer rim of the data lens down to the metal tube. This reduced the shadow enough to make the outer reseau cross visible at all of the camera settings under consideration.

Before final assembly into the camera, the metal surfaces of the data assembly were painted with flat-black paint to minimize unwanted reflections. The stop was positioned about 2.5mm in front of the data lens and held in place by the paint. The mounting plate of the assembly was securely taped in position both with double-backed and with black photographic tape. The completed data system assembly is shown in the photographs of Figures 3 and 4.

Figure 3. Installed data system, rear view.

Figure 4. Installed data system, front view.

B. Initial Evaluations

With the completion of the data system assembly, it then became possible to evaluate the performance. The visual appearance of the data image was quite acceptable; the edges were generally sharp and the response to camera focus and aperture changes was very detectable. The vignetting shown in the image at camera apertures larger than f/11 was very striking and resulted from two different sources. The vignetting of the inner-edge was found to be the image of the vignetted iris in the camera lens; that of the outer-edge was vignetting caused by an insufficient clear aperture for the data lens itself. Neither form of vignetting is overly detrimental to the data system. The shadow from the data lens assembly was nicely restricted to the picture area bounded by the outer reseau cross and the frame corner. Only at the camera apertures of f/16 and smaller does the shadow begin to obscure the outer reseau cross.

The data system is complete only when an acceptable photographic image can be produced with the films used on the lunar surface. Currently, a high speed color reversal film, Kodak SO168, and a high speed black and white film, Kodak SO267, are being used.[13] Both of these films are coated on thin Estar base material in 70mm widths and each camera film magazine can contain as much as forty feet of either film type. Because of the relative simplicity of processing black and white emulsions, short sections of the SO267 film were used to obtain preliminary photographic evaluations of the data system.

The illumination source used for these early evaluations and for the system calibration runs to be discussed in the next subsection was a Kodak Adjustable Safe-Light with a 15 watt tungsten lamp and an opal glass front cover. When the camera lens was placed against the opal glass, diffuse illumination was provided over the entire camera field of view. The following exposure technique was used to simulate the lunar surface operational situation where the variation in scene luminance is compensated for by camera aperture changes. The camera shutter speed was adjusted to produce an average photographic exposure of the frame for the unfiltered diffuse source and the f/16 aperture setting. Neutral density filters were placed between the opal glass and the camera lens for the other aperture settings as follows: f/11 - .3ND, f/8 - .6ND, and f/5.6 - .9ND. In this way, the average frame exposure remained constant and the equivalent scene luminance was a maximum at f/16 and a minimum at f/5.6. Since the data image illuminance is proportional to the scene luminance, the data image exposure increases with scene luminance when the exposure time is constant. Figure 5 is a typical density versus log-exposure curve showing the data image densities relative to that of the frame center. This relative relationship can be adjusted, as described earlier, by changing the stop diameter of the data lens assembly. The data of Figure 5 indicates that the stop of this particular system corresponds to a compromise camera aperture value of approximately f/9. This configuration provides a nearly balanced data image ex-

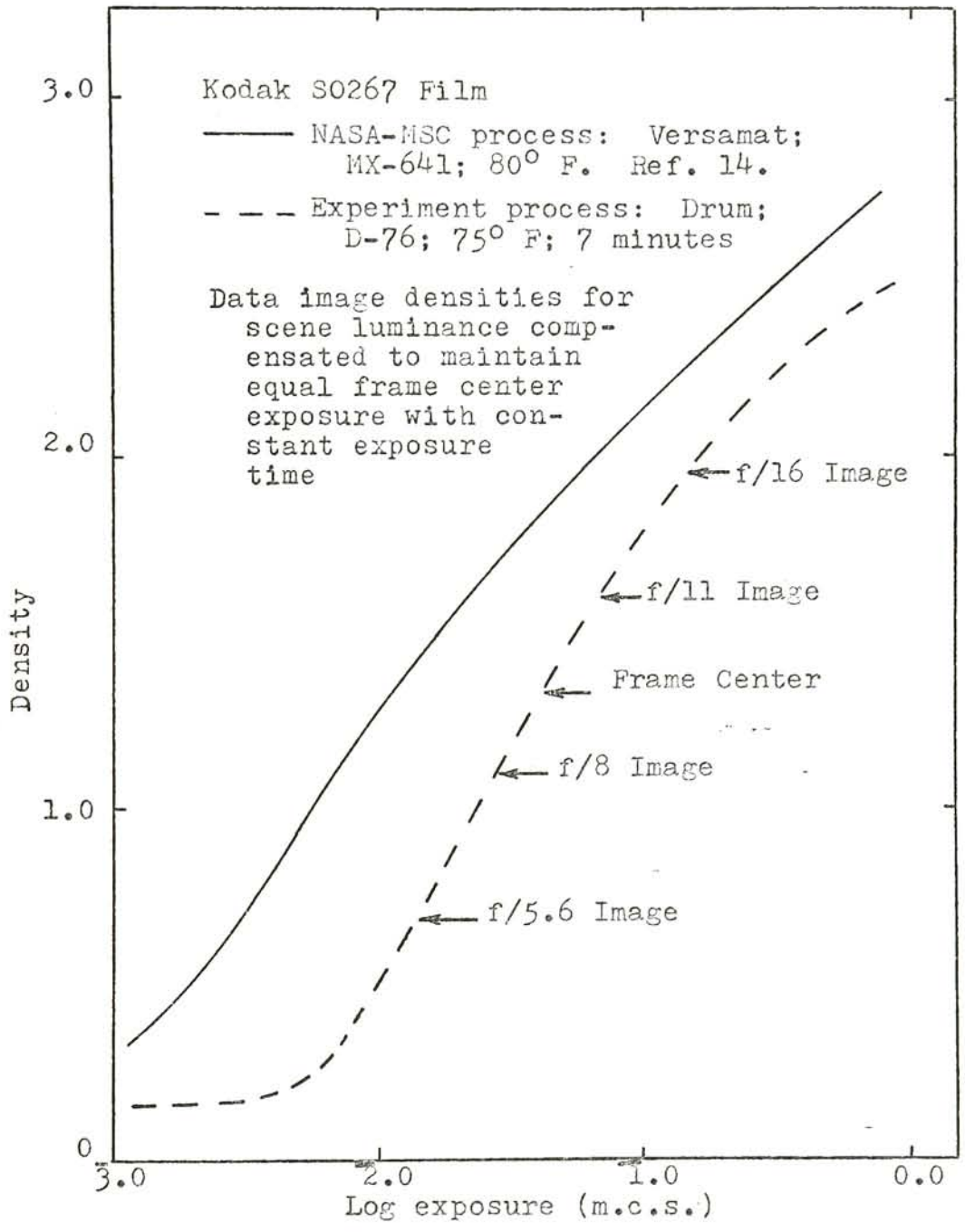

Figure 5. Relative sensitometric properties of the data system.

posure range for the camera aperture settings in question.

Processing of the S0267 film was accomplished using a Kodak Rapid Color Processor, Model 11, with E-76 developer at 75° F for seven minutes. Two film strips no longer than 22 inches each can be processed at the same time. The stop and fixing portions of the process also were performed using the machine, but a deep tank was used to insure uniform washing. A typical sensitometric curve for NASA's Kodak Versamat processing of S0267 using MX-641 chemistry at 80° F is shown in Figure 5 for comparison.[14] The large speed difference of the two processing methods results from differences in the developer activity and the spectral characteristics of the sensitometry. The preliminary nature of the system evaluation did not warrant any better duplication of the NASA results.

Typical data images for several aperture and focus combinations are shown in Figure 6 and clearly indicate the ranges of image shapes and positions. The pentagonal shape of the camera iris and the vignetting discussed earlier are quite apparent from these images and a measurement technique had to be developed around these image characteristics. A sharp circular image would provide an ideal measurement source because it would be very easy to locate the image center for focus determinations and to measure the image diameter for aperture indication.

Figure 7 diagrammatically shows the measurement technique finally decided upon for the actual images.

Figure 6. Typical data image shapes.

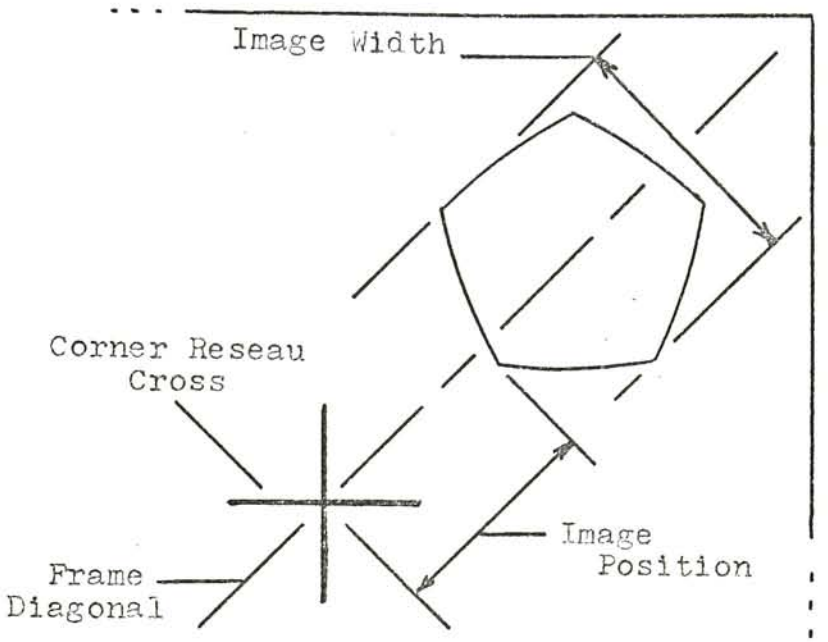

Typical Non-Vignetted Image

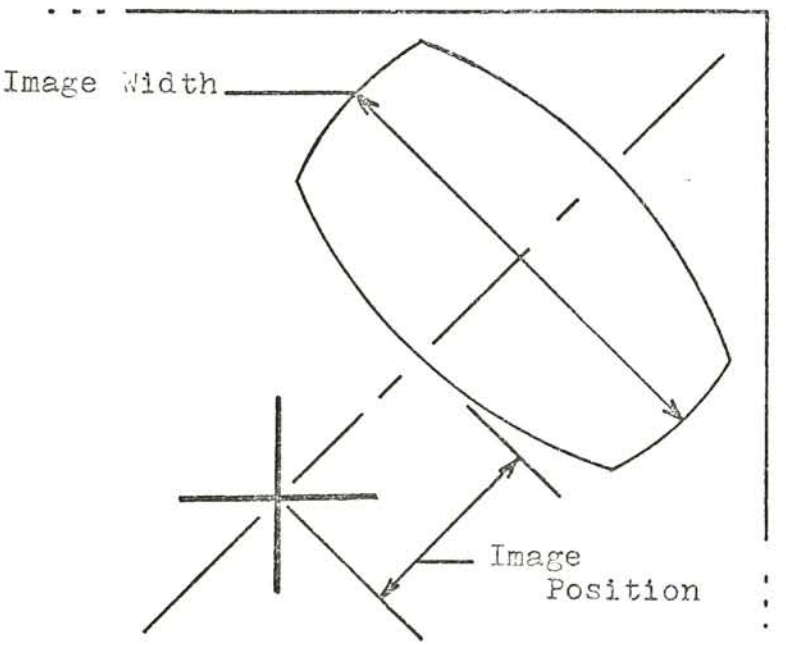

Typical Vignetted Image

Figure 7. Image measurement technique.

The measurement coordinate system is Cartesian and based upon the camera frame diagonal. Position measurements are always determined along the diagonal from the reseau cross to the innermost edge of the image. This technique has the disadvantage of unnecessarily including aperture dependence in the position value, but it eliminates any requirement to use the outer image edge which often is made very indistinct by the vignetting of the data lens. The width of the data image always is determined as the maximum extent of the image along a line perpendicular to the frame diagonal.

C. System Calibration

Each operational data system would require an image calibration before aperture and focus determinations could be made for actual field photographs. In order to investigate what should be included in operational calibrations and to determine the more detailed characteristics of this trial system, a straightforward calibration of the system was performed as described in detail in Appendix B. The five focus values of 3, 5d (detent), 8, and 15d (detent) feet and infinity (detent) were used along with the five aperture values of f/5.6, f/8, f/9.5, f/11, and f/16. These values produced twenty-five combinations that were exposed in random order. The tungsten illumination source and filtered exposure technique described in the previous subsection were used throughout. Six complete exposure sequences were made on each of the two film types and the film processing was performed by the NASA Photographic Technology Laboratory in Houston to the normal Apollo flight standards.

Image measurements were made according to the guidelines described in the previous subsection. A Quality Evaluation Viewer, Model IV, measurement light table, manufactured by Photogrammetry Inc. and having x and y axis micrometers marked in 0.002mm per division, was used in making the measurements. The images were viewed under 32x magnification, and multiple measurements were obtained as described in Appendix B. The results of the calibration are presented in section IV.

D. System Field Tests

In order to obtain some realistic examples with which to test the usefulness of the calibration results, a large number of photographs were obtained with the camera system on and around the Rochester Institute of Technology campus. Once again, both films were used and the processing was done by NASA. Every half-stop from f/5.6 to f/16 and the focus settings of 3, 3.5, 4, 5d, 6, 8, 10, 15d, 30, 70d feet and infinity were used. Exposure combinations were made by randomizing independently the aperture and the focus settings and a variety of scenes were used. Image measurements were obtained in the same manner as for the calibration and the results are presented in the following section.

IV. RESULTS

IV. RESULTS

All of the calibration and field test photographs resulted in usable examples of the data system operation; however, it was not necessary to use them all in order to describe the system sufficiently. The specific results obtained from evaluation of the data images are presented in the following subsections.

A. System Calibration

The primary objective of system calibration is to determine what, if any, functional relationships exist between the aperture and focus settings and the data image width and position measurements. This determination was made using only four of the six black and white exposure sequences and the standard statistical techniques as described in Appendix B. Figure 8 is a graphical presentation of the relationships found to exist between the data image position and the camera focus setting. The curves are the statistical results obtained by polynomial regression of the measurement data. The position relationships are also functions of the camera aperture setting as a result of the measurement technique; however, a single positional relationship exists for the aperture settings of f/5.6 through f/8 because of the iris vignetting in the camera lens. In these vignetted cases, the inner edge of the data image actually is the image of the vignetting structure in the lens and is, therefore, independent of the lens iris. The slightly higher slope of the curve for the vignetted settings results from the fact that the vignetting surface is

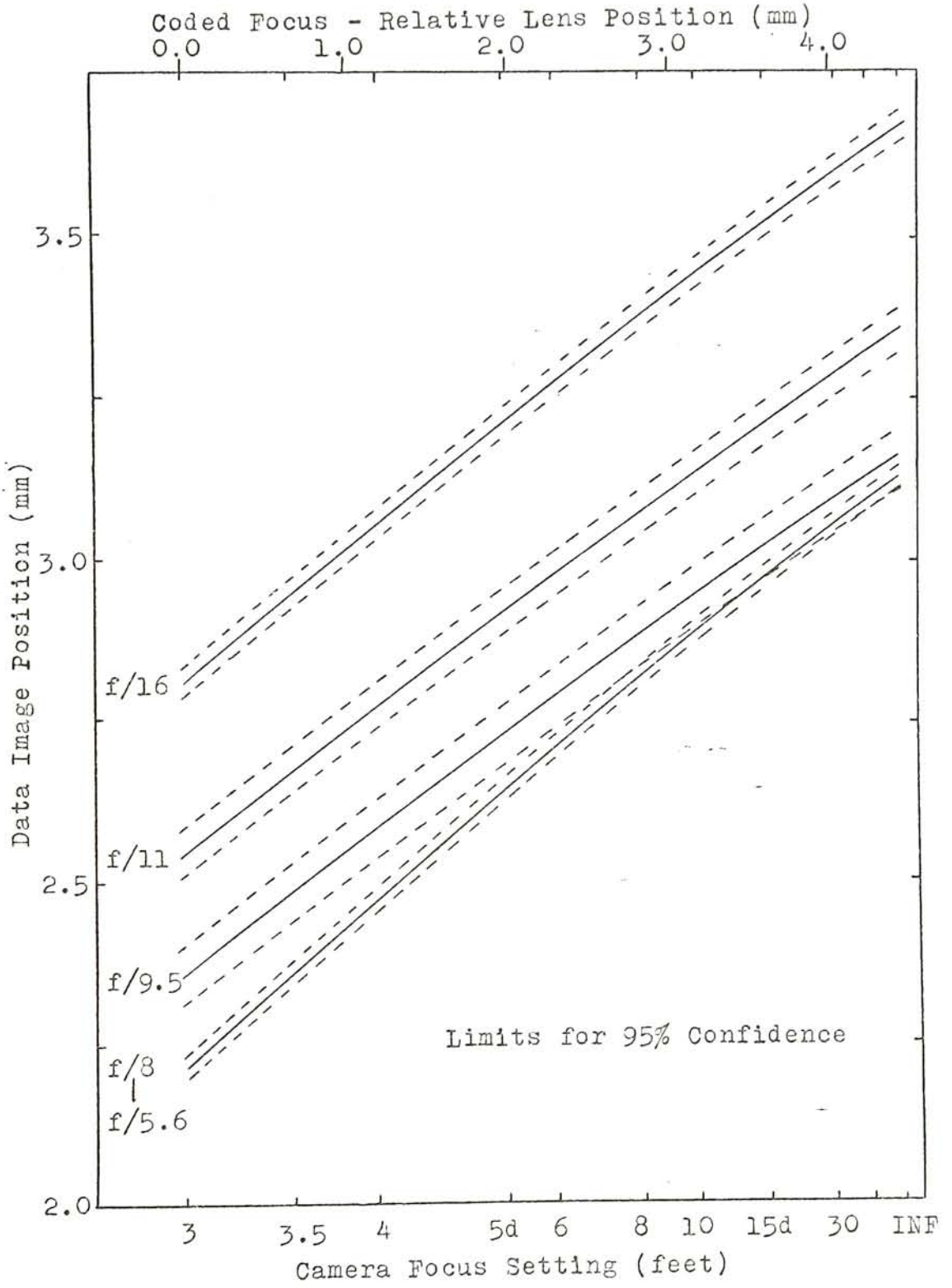

Figure 8. Data image position versus camera focus and aperture settings.

closer to the data lens than is the camera iris.

The graphical relationships of the image width and the camera aperture and focus settings are shown in Figure 9. The dual dependence of the width on both aperture and focus was predicted by the theoretical considerations. The statistically determined relationships for width are more strongly quadratic than those for position, as clearly shown in Appendix B. Figures 8 and 9 are then the calibration curves for this data system when the black and white film is used.

The measures of data system variability, determinable from the calibration data, almost equal the importance of the functional relationships. The statistical treatment of the measurements must be considered carefully in order to separate properly the sources of variation. Appendix B demonstrates the analysis techniques used in this investigation where a total of 400 measurements had to be considered.

The first indication of how the data should be subdivided for analysis came from the obvious variation differences between aperture settings. However, even when the data was grouped according to the aperture settings, the basic measurement variations were statistically equal and could, therefore, be pooled to a single value. The derived overall measurement precision based on 200 pairs of measurements is shown in Table 3.

The position measurements for the vignetted aperture values of f/5.6 through f/8 provided a unique way to determine the variation associated with repositioning the camera focus ring because of the aperture independence of

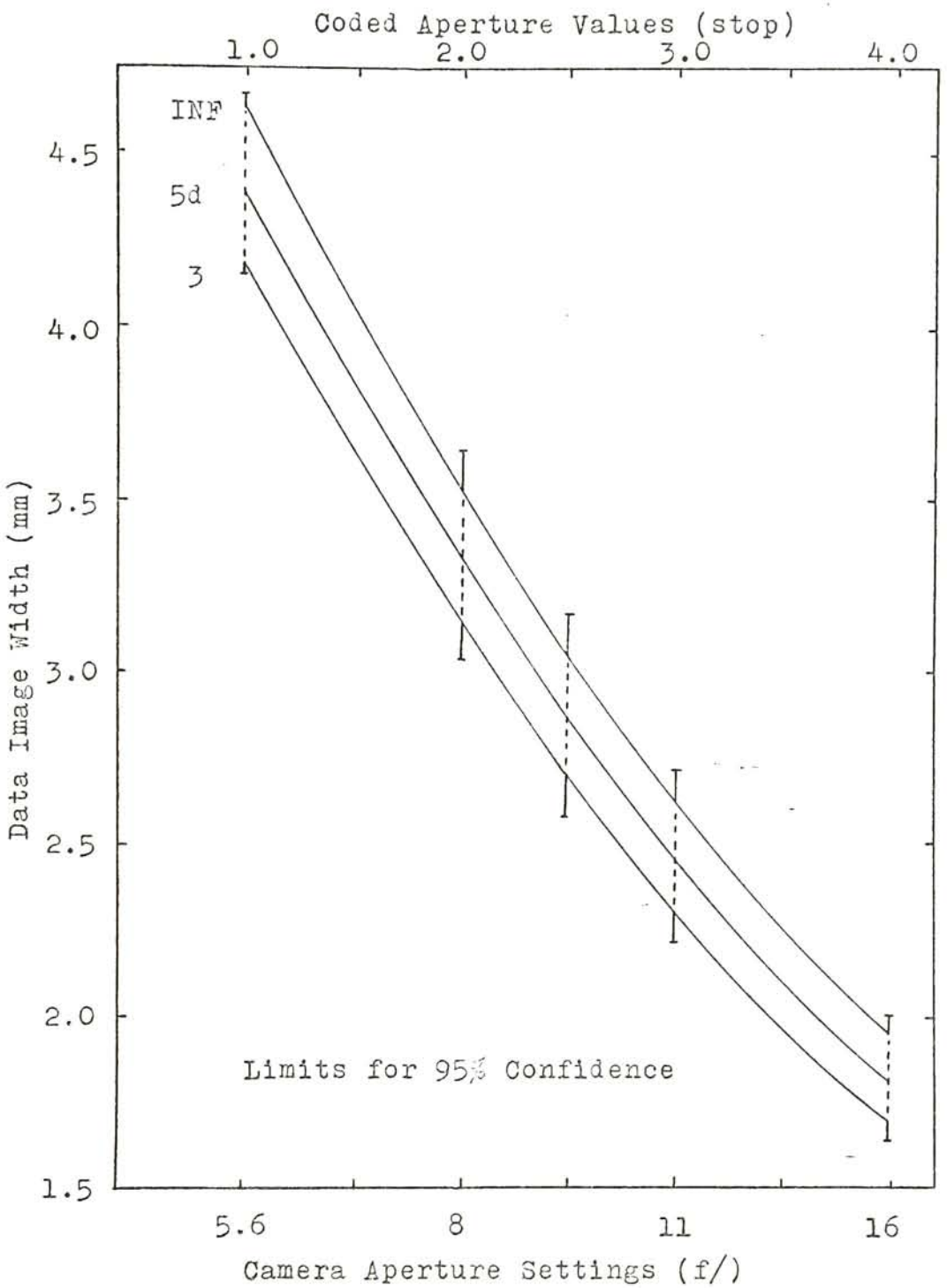

Figure 9. Data image width versus camera aperture and focus settings.

Table 3. Itemized variability from system calibration

Source of Variation	95% Confidence Limits (mm)	
a. Between measurements	0.0040	0.0048
b. Between like focus settings	0.0000	0.0048
c. Between position measurements at f/9.5	0.0137	0.0374
d. Between position measurements at f/11	0.0107	0.0290
e. Between position measurements at f/16	0.0000	0.0067
f. Between width measurements at f/5.6	0.0000	0.0029
g. Between width measurements at f/8	0.0320	0.0857
h. Between width measurements at f/9.5	0.0364	0.0973
i. Between width measurements at f/11	0.0271	0.0723
j. Between width measurements at f/16	0.0029	0.0103
k. Error about regression for position measurements	0.0044	0.0085
l. Error about regression for width measurements	0.0043	0.0158

Table 4. Predicted camera iris variability

Aperture	Iris Diameter[11]	% Diameter Change	% Area Change
f/8	7.7mm	5.6%	11.2%
f/9.5	6.6mm	7.4%	14.9%
f/11	5.6mm	6.5%	13.0%
f/16	3.8mm	1.5%	2.9%

these particular measurements. The results are shown in Table 3, and clearly indicate that the variation due to focus setting is not significantly different from that of pure measurement precision. This is a very important result because it means that the remaining variability in the data is a result of variations in the camera iris itself. This result also justifies the initial grouping of the data by aperture value.

The variations in the remaining position data can be attributed to the iris variability induced through the measurement technique. This supposition is substantiated further by the fact that the width variability shows the same magnitude trends as does the position variation for like aperture values.

The width variation data can be considered a direct result of variability in the camera iris positioning mechanism. As Table 3 shows, the width variations are much larger generally than that of the position measurements. The insignificantly small variation in the width measurements for the f/5.6 settings is to be expected when it is realized that the lens internal structure actually becomes the aperture for this setting. The iris diaphragm for f/5.6 opens to a larger diameter than that of the maximum clear aperture of the lens; therefore, no iris variability can enter into the f/5.6 width measurements.

As shown in Appendix B, the variations in data image width can be converted directly to measures of lens iris variability. By considering the resultant data system magnification and the exit pupil dimensions furnished in reference 11, percentage changes in camera

aperture diameter and area can be determined for this particular camera. The calculated values for the camera iris variations are presented in Table 4, based on the upper 95% confidence limits from Table 3.

The appropriate combinations of the variations must be used to place confidence limits on the values of position and width for the various aperture and focus settings. This has been done in Figure 8 with dashed lines and in Figure 9 with bars for 95% confidence. Since no data was obtained for the f/6.7 or the f/13.2 settings, no variability limits can be made for these values even-though the functional relationships can determine their basic image measurements. This then becomes a calibration deficiency that can be corrected only by using all the aperture values during calibration. This improved calibration method also would provide the much needed position versus focus curve for f/13.2.

B. System Field Tests

With the data system calibration completed, it should be possible to determine what the field test settings were, based on the functional relations found during calibration. An examination of Figures 8 and 9 reveals that neither aperture nor focus can be resolved independently because of the variability in the system resulting primarily from the camera iris variations. An important fact concerning the iris variations is that they exist even without the data system installation and that a perfect external record of the aperture settings still would be limited by this same iris variability. Since the data image is a permanent record of what the actual

iris condition was at the time of the photograph, the data system provides a means of eliminating the iris variability effects. The recording qualities of any specific data image are, therefore, limited by only the measurement and regression errors of the data system; as shown in Table 3, these errors are noticeably smaller than those of the iris.

To make use of the above principle and to provide an efficient means of determining camera settings from image measurements, a Fortran IV computer program was developed and is described in Appendix C. This program is based on the black and white calibration data analyses and uses iterative techniques, with both the width and the position measurements for an image, to calculate the most probable camera settings. The equations used in the program are derived from the exact regression equations of the calibration data and the equivalent regression errors for the program are slightly larger than those reported in Table 3 for the calibration. The program places 95% confidence limits on the best values by taking into consideration both the measurement and the equivalent regression errors. When the program is run using the calibration data, the results are very good with the deviations being normally distributed and primarily larger at the higher focus and aperture values.

One-hundred of the black and white and twenty-five of the color field test data images were measured using the same technique as described in section III, C.

However, since measurement precision had been well established during the system calibration, only one value for each image parameter was obtained for these field test measurements. It also should be noted that the black and white field test images generally were overexposed by about a stop; however, the data images appeared quite usable with only a slight decrease in edge sharpness being noticed.

The field test image measurements were translated into focus and aperture values by using the computer program described in Appendix C. When the focus results are compared with the values recorded during the photography, the calculated focus limits include the target value in 27% of the black and white frames and in 52% of the color frames measured. When the black and white and the color images are considered together, 32% "success" is obtained. A conspicuous feature of the data, as shown in Appendix D, is that a significant bias to lower focus values exists throughout. This bias is equivalent to position measurements that on the average are 30 micrometers short. Eventhough no significant cause for this bias can be determined from the data, chromatic aberration effects or mechanical changes in the data lens system could have provided this bias.

The ability to differentiate between various focus settings is a more meaningful measure of the quality of the data system. The calculated focus ranges for each target setting are shown in Table 5, along with a symbolic representation of which settings are resolvable.

Table 5. Maximum calculated focus ranges and resolvable settings from field test images

Target Focus(ft)	Maximum Calculated Range(ft)
3	2.8 - 3.0
3.5	3.3 - 3.6
4	3.7 - 4.1
5(detent)	4.6 - 5.4
6	5.2 - 6.3
8	6.5 - 8.6
10	7.4 - 12.7
15(detent)	10.1 - 15.8
30	16.3 - 36.9
70(detent)	19.4 - 141.1
Infinity	24.0 - 1067.2

Resolvable Settings:

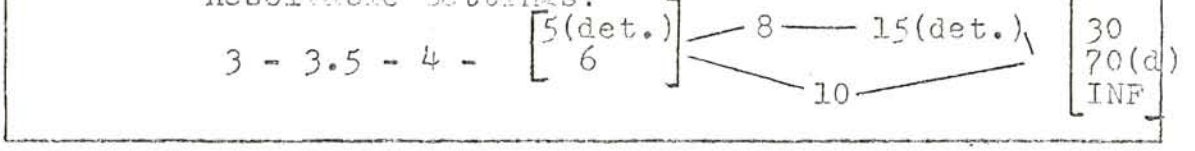

Table 6. Maximum calculated aperture ranges from field test images

Target Aperture (f/)	Maximum Calculated Range (f/)
5.6	5.5 - 5.8
6.7	6.2 - 6.8
8	7.5 - 8.4
9.5	9.1 - 10.0
11	10.6 - 12.1
13.2	12.7 - 14.3
16	15.1 - 17.4

This presentation clearly shows that more settings can be distinguished than had been hoped at the beginning of this investigation.

When the aperture results are compared with the recorded values, 50% of the black and white and 52% of the color frames contained the target value within the calculated limits. Only a slight low bias could be detected and this probably results from regression effects at the low aperture values. That the limits contain the recorded aperture setting value is not the goal nor is to be expected because of the inherent wide ranges of the camera iris. The aperture range determined with the field test data and shown in Table 6 reveals that each half-stop target value can be resolved by this data system. The ranges are distributed evenly about the target values except for those at f/6.7 and f/5.6. Since no calibration data was obtained for f/6.7, there is a good possibility that the functional relationships from width calibration do not determine the large aperture values as well as expected.

The aperture range calculations for black and white frame number 59 were discounted because of the speculative nature of the image measurements. This case emphasizes the detrimental effects of having deep-shadows imaged by the camera in the area of the data image. Either the reseau cross, the data image, or both can be rendered undetectable because of the shadow effects. This frame, along with several other examples of field test data, is shown in Figure 10.

9: f/11, 30 ft.

4: f/16, INF

58: f/9.5, 70d ft.

59: f/8, 8 ft.

99: f/8, 15d ft.

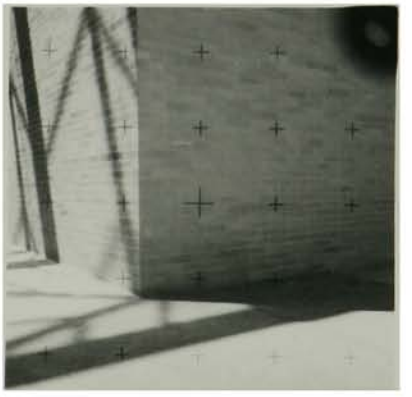

84: f/6.7, 6 ft.

Figure 10. Representative black and white field test frames.

V. DISCUSSION

V. DISCUSSION

The above results, obtained with a rather crude data system design, clearly indicate that meaningful determinations of camera aperture and focus settings are possible with this optical technique and camera. The initial objectives of this research have been met and, in addition, it has been shown that valuable measures of the camera iris variability can be obtained as a by-product.

An operational data system could be improved in several ways. First of all, the data lens design should provide better optical correction of chromatic aberration, astigmatism, and internal vignetting. Furthermore, the data lens assembly should be rigidly mounted to the camera and more precisely aligned and focused. For use on the lunar surface, where the black of space becomes the "sky" of the picture, the data image should be located in one of the upper corners of the camera image plane where the lunar surface would become the image background. Even when this is done, the data image may be lost when a deep shadow area of the lunar surface is imaged on the data image location.

The results of the system field test evaluation indicate that the calibration obtained from the black and white film is sufficient to determine the data system results both for the black and white and the color film. Therefore, the number of calibration exposures can be reduced by at least one-half. Since the primary variability of the data system results from the camera iris, all of the detented aperture settings in the range of interest should be used. This would increase the number of aperture levels to seven for the range of f/5.6 to f/16. Since the focus variability is insignificant, the focus levels used in calibration could

be reduced to four. While this improved calibration design would increase the number of required exposure combinations by only four, it would provide measures of variability for all of the aperture settings. Furthermore, an independent measure of the actual aperture values should be made to insure that the functional relationships are derived correctly. All of these calibration improvements could result in better operation of the computerized evaluation program. A basic improvement of the calibration technique, that should have been recognized earlier in this research, would be to use an illumination source that is more representative of the spectral composition of the field illumination.

Once an improved data system is available, the effects on the data image from using different film magazines should be investigated. The intended interaction of the reseau plate rims and the film magazine pressure plate should prohibit any magazine effects for this camera design. Likewise, the effects of removing and reinstalling the camera lens should be studied. Since the photogrammetric calibration of the camera depends upon the repeatability of this lens mounting, very little variation in the data system should result from this factor.

The possibility of using the data system to determine the actual aperture setting to closer tolerances than would be permitted with a perfect written record was not evaluated in detail because of the possible aperture data contamination from the position bias. The practicability of this concept, however, is based on the statistics of the

system and only requires that the combined measurement and equivalent regression errors be less than those of the iris variability.

VI. CONCLUSIONS

VI. CONCLUSIONS

With a relatively simple optical data system and system installation, it has been shown that, for the lunar surface camera and films tested in this research, the following conclusions are justified.

(1) The optical data system can record lens aperture settings resolvable to the half-stop values in the range of f/5.6 to f/16 with at least 95% confidence.

(2) The data system can be used to distinguish between the focus settings in feet of 3, 3.5, 4, 5d, 8, 15d, and 70d with 95% confidence.

(3) The data system calibration can provide a measure of the camera iris variability to high levels of confidence.

Furthermore, since the theoretical basis is general in nature, this optical recording technique may be usable in other camera designs, especially where a record of the iris characteristics is desired.

REFERENCES

1. R. E. Thompson, "A 2½ by 2½ Inch Photogrammetric Camera System for the Moon." New Horizons in Color Aerial Photography (Seminar Proceedings), SPSE, p. 175, June, 1969.

2. T. Rindfleisch, "Photometric Method for Lunar Topography," Photogrammetric Engineering, Vol. 32, p. 262, March, 1966.

3. B. Hallert, "Photogrammetry," New York: McGraw-Hill Book Company, Inc., 1960.

4. R. M. Batson, "Photogrammetry with Surface-Based Images," Applied Optics, Vol. 8, p. 1315, 1969.

5. Military Standardization Handbook, "Optical Design," MIL-HDBK-141, 1962.

6. W. J. Smith, "Modern Optical Engineering," New York: McGraw-Hill Book Company, Inc., 1966.

7. A. Cox, "A System of Optical Design," New York: Focal Press Limited, 1964.

8. NASA-Manned Spacecraft Center Drawings, SEB33100040 and SEB33100048, Houston, Texas.

9. Victor Hasselblad AB Drawings, Nr. 70-1011/IV and Nr. 70-1012/D/I, Göteborg, Sweden.

10. Carl Zeiss Drawing, 10 63 01 V1-0001(3), Oberkochen, West Germany.

11. H. Sauer, Carl Zeiss Letter, Oberkochen: January 12, 1970.

12. A. E. Conrady, "Applied Optics and Optical Design," New York: Dover Publications, Inc., Part II.

13. W. N. Teague, "Final Photographic and TV Procedures, Apollo 13," Houston: NASA - Manned Spacecraft Center, April 3, 1970.

14. R. W. Underwood, NASA Letter, Houston: April 3, 1970.

15. A. D. Rickmers and H. N. Todd, "Statistics: An Introduction," New York: McGraw-Hill Book Company, Inc., 1967.

16. A. J. Duncan, "Quality Control and Industrial Statistics," Homewood, Ill.: Richard D. Irwin, Inc., 1959.

17. N. R. Draper and H. Smith, "Applied Regression Analysis," New York: John Wiley and Sons, Inc., 1968.

APPENDICES

APPENDIX A

Optical Design

A. First-Order (Thin-Lens) Considerations

The optical layout of the lunar surface camera is shown clearly in Figures 1a and 1b of the text, and the necessary optical dimensions and parameters are as follows:

(1) Camera lens focal length = 61.49mm

(2) Camera pupil to reseau plate distance -
for 3 feet focus = 61.82mm
for infinity focus = 57.39mm

(3) Reseau plate thickness = 4.00mm

(4) Reseau plate indices of refraction (Schott glass BK7): $N_f = 1.52238$, $N_d = 1.51673$, $N_c = 1.51432$

(5) Reseau plate to film plane distance = 0.10mm

(6) Exit pupil diameter for f/5.6 = 11.01mm

The camera focal length (1) is the calibrated focal length supplied with the particular camera used in this experiment and the other dimensions are from references 8, 9, 10, and 11.

The most convenient measure of camera focus is not the setting value, but is rather the actual lens displacement in millimeters from some reference focus setting. This displacement can be obtained by assuming the Gaussian image equation for the camera object and image distances, i.e.,

$$\frac{1}{\text{camera focal length}} = \frac{1}{\text{object distance}} + \frac{1}{\text{image distance}}$$

If the focus setting values are used as object distances, then the resulting image distances are specified as listed in Table A-1.

Table A-1. Camera focus dimensions

Focus Setting(ft.)	Pupil to Plate(mm)	Change from 3 ft.(mm)
3	61.823	0.000
3.5	61.151	0.672
4	60.656	1.167
5	59.975	1.848
5(detented)	59.847	1.976
6	59.529	2.294
8	58.981	2.842
10	58.656	3.167
15(detented)	58.223	3.600
30	57.806	4.017
70(detented)	57.559	4.264
Infinity	57.390	4.433

Much of the optical design of the data system was optimized for the 5 feet focus setting. When the physical dimensions for this focus are used, the distance from the (thin) data lens to the reseau plate as a function of the data lens focal length is shown in Figure A-1. This figure also demonstrates the optical and the physical limitations for the maximum data lens focal length.

The camera dimensions can be used with the data lens focal length to calculate the data system magnifications as presented in Figure A-2. Large magnification differences with camera focus are required for focus detection, and it is clear from this figure that the larger the data lens focal length, the better this goal is met.

The magnification of the data system must be limited to a value that will produce a data image of reasonable size. If the image is to be confined to the area between the outer reseau cross and the frame corner, then Figure A-3 indicates the data system parameters that can be used. Data image

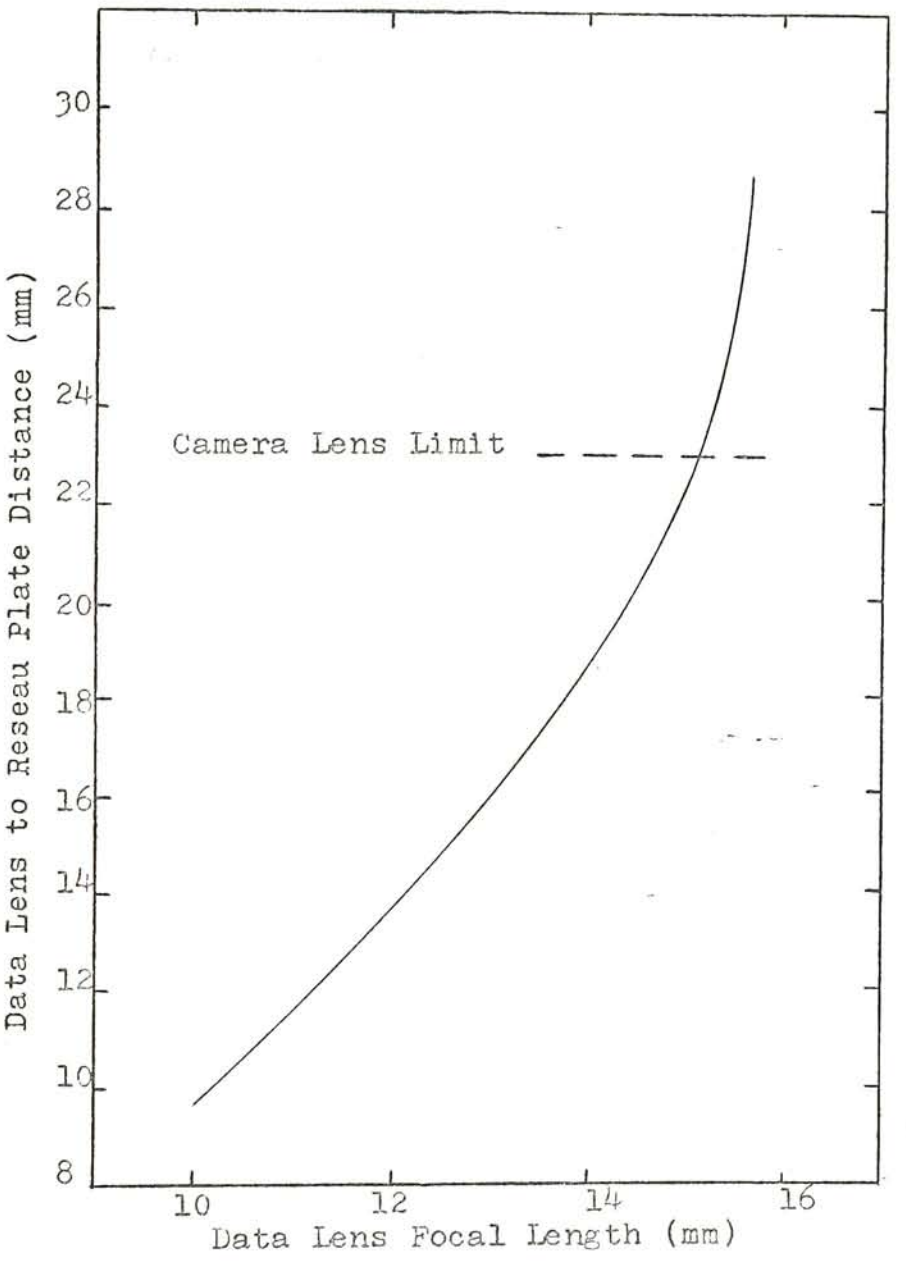

Figure A-1. Data lens to reseau plate distance versus data lens focal length.

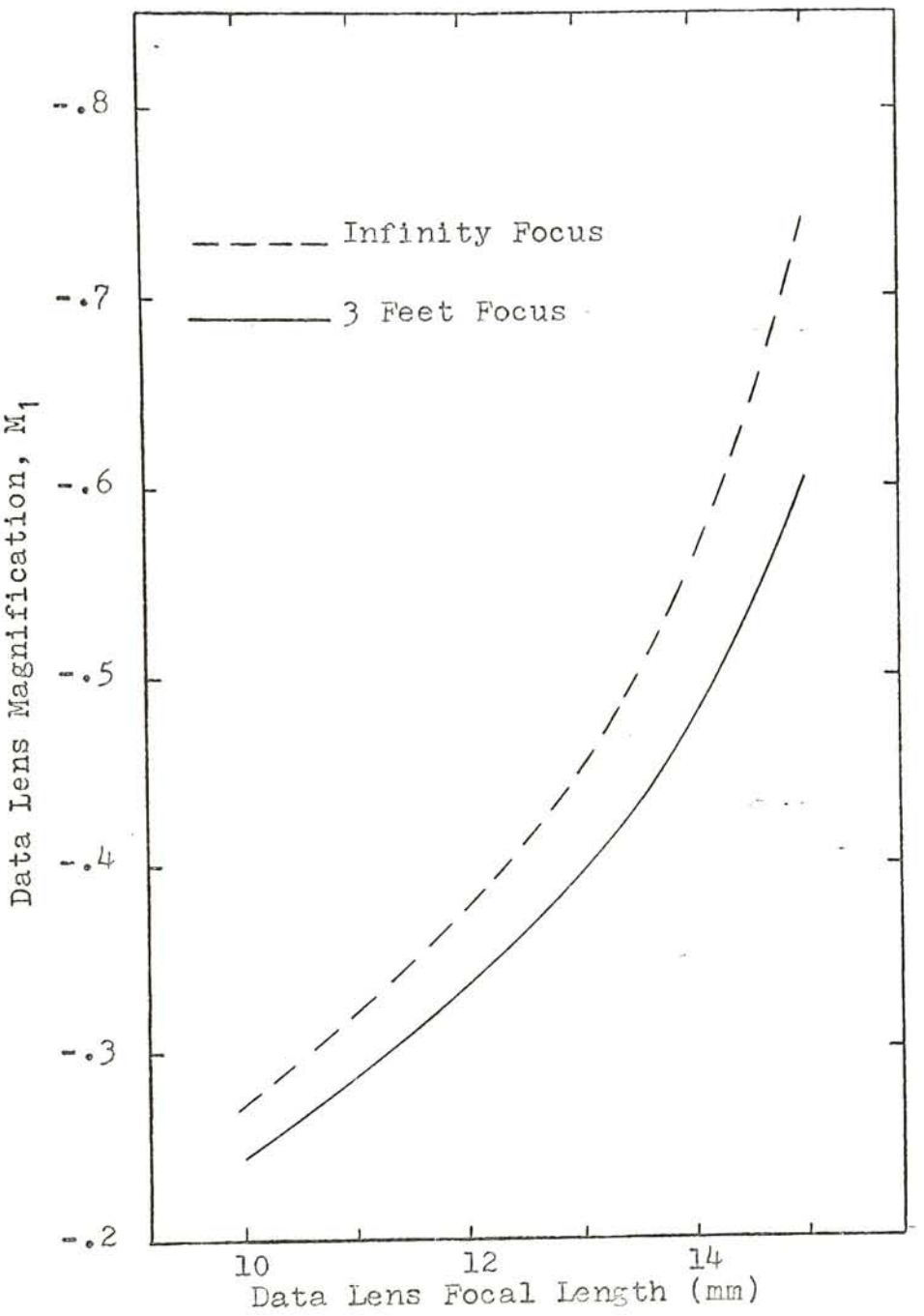

Figure A-2. Data lens magnification versus focal length.

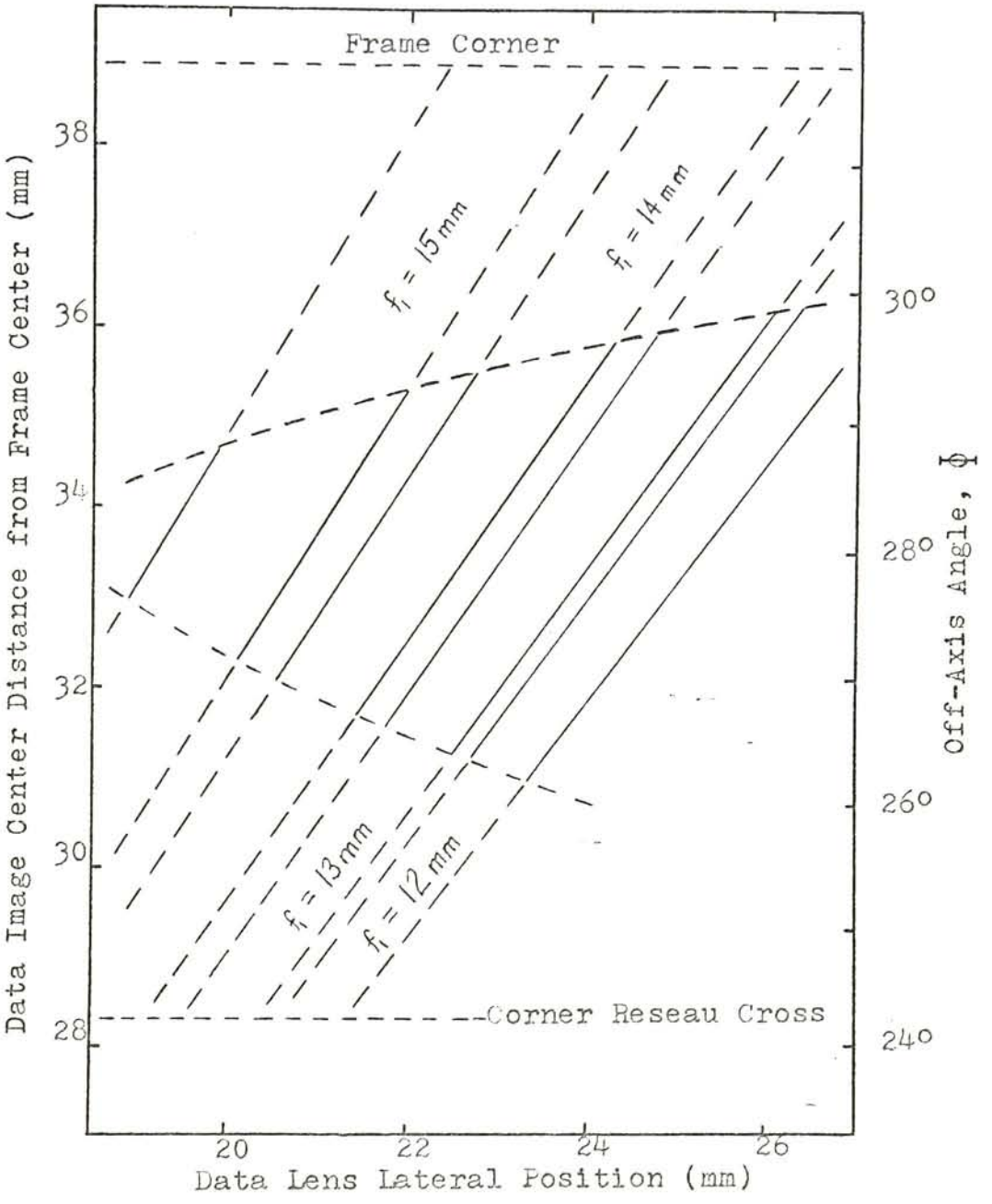

Figure A-3. Data system parameter envelope.

size is the primary restriction and the limits shown are those that permit the complete data image to be recorded without losing the reseau cross. For maximum magnification and a sufficiently small data image, a 14mm focal length is the indicated limit. It is interesting to note that the experimental data system, in effect, widened these calculated limits by decreasing the image length through the vignetting that actually occurred.

B. Third-Order Considerations

The effects on the proposed data system from third-order aberrations were obtained through the use of the optical design programs of the Royal McBee, LGP-30, electronic computer. The actual tracing of rays through the data system for final system evaluation also was performed with these programs.

The initial task was to evaluate the effects of changing the surface curvatures of the data lens while maintaining the desired lens focal length and image location. For a fixed focal length and lens thickness, one curvature is dependent upon the other. Figure A-4 shows the effects on astigmatism, coma, and spherical aberration from "bending" the first surface curvature of a 12mm focal length data lens. For reduced astigmatism, a negative miniscus lens design is indicated, but it is evident that the spherical aberration coefficient increases for this case. The coma can be removed by proper location of the data system aperture stop as shown in Figure A-5. It should also be noted that the astigmatism for this coma-free stop position is reduced greatly over the equivalent plano-convex design with the stop at the lens.

Once the plano-convex lens with the shifted stop had been

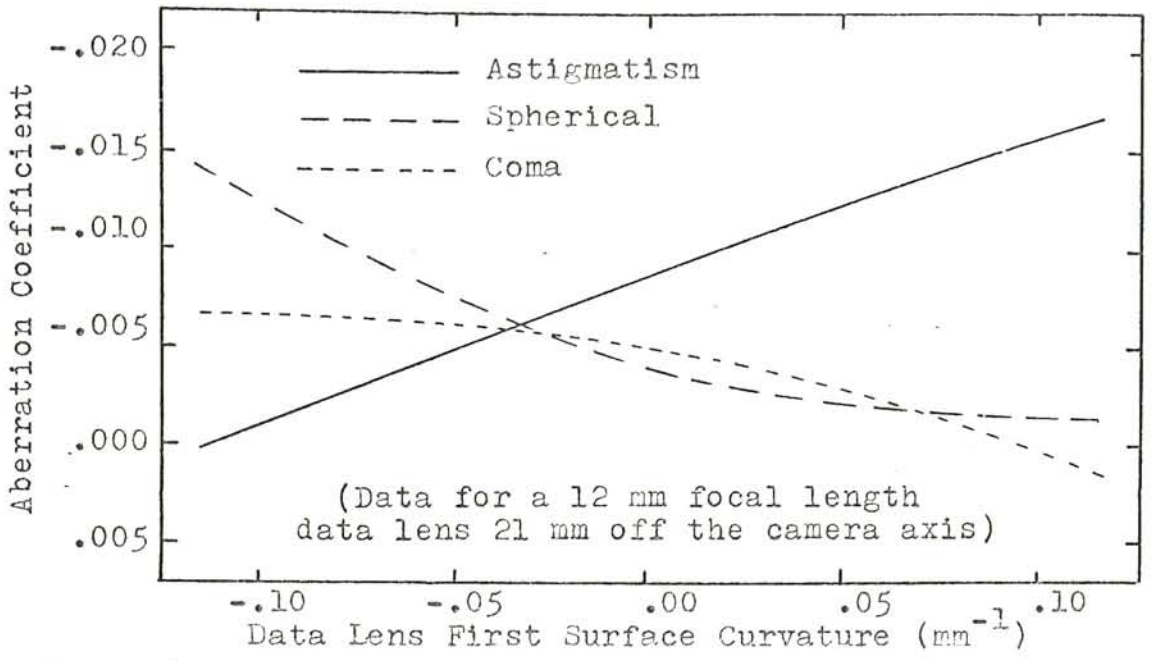

Figure A-4. Surface curvature effects on astigmatism, coma, and spherical aberration.

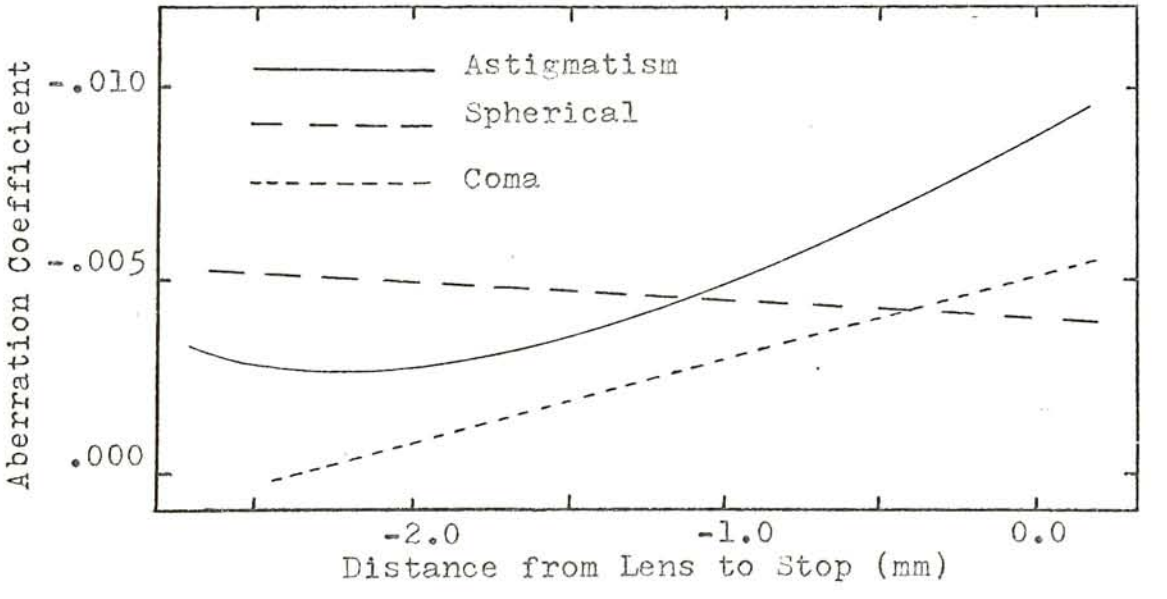

Figure A-5. Stop-shift effects for a plano-convex data lens.

decided upon, the remainder of the design task involved refining the system focus location and evaluating the image quality. Since the design still possessed some astigmatism, it was possible to optimize the system focus for either the tangential or the sagittal conditions. Table A-2 provides the system parameters and resultant aberrations for the tangential, Case 77, and the sagittal, Case 78, focus situations. Figure A-6 shows the tangential and sagittal ray intercept curves for these two cases when the camera is focused at 5 feet. The shapes of the curves changed very little with camera focus.

Table A-2. System parameters and aberrations for tangential and sagittal focus

Characteristic	Tangential Focus (Case 77)		Sagittal Focus (Case 78)
Pupil to stop distance	43.8597mm		43.6682mm
Stop diameter		2.000mm	
Stop to 1st surface		2.300mm	
1st surface curvature		$0.000mm^{-1}$	
1st to 2nd surface		2.500mm	
2nd surface curvature		$-0.161mm^{-1}$	
2nd surface to reseau	11.3156mm		11.5071mm
Reseau plate thickness		4.000mm	
Plate to film distance		0.100mm	
Film to axial focus	1.9934mm		1.8236mm
Lens focal length		12.014mm	
Spherical aberration		-0.0050	
Coma		-0.0001	
Astigmatism		-0.0026	

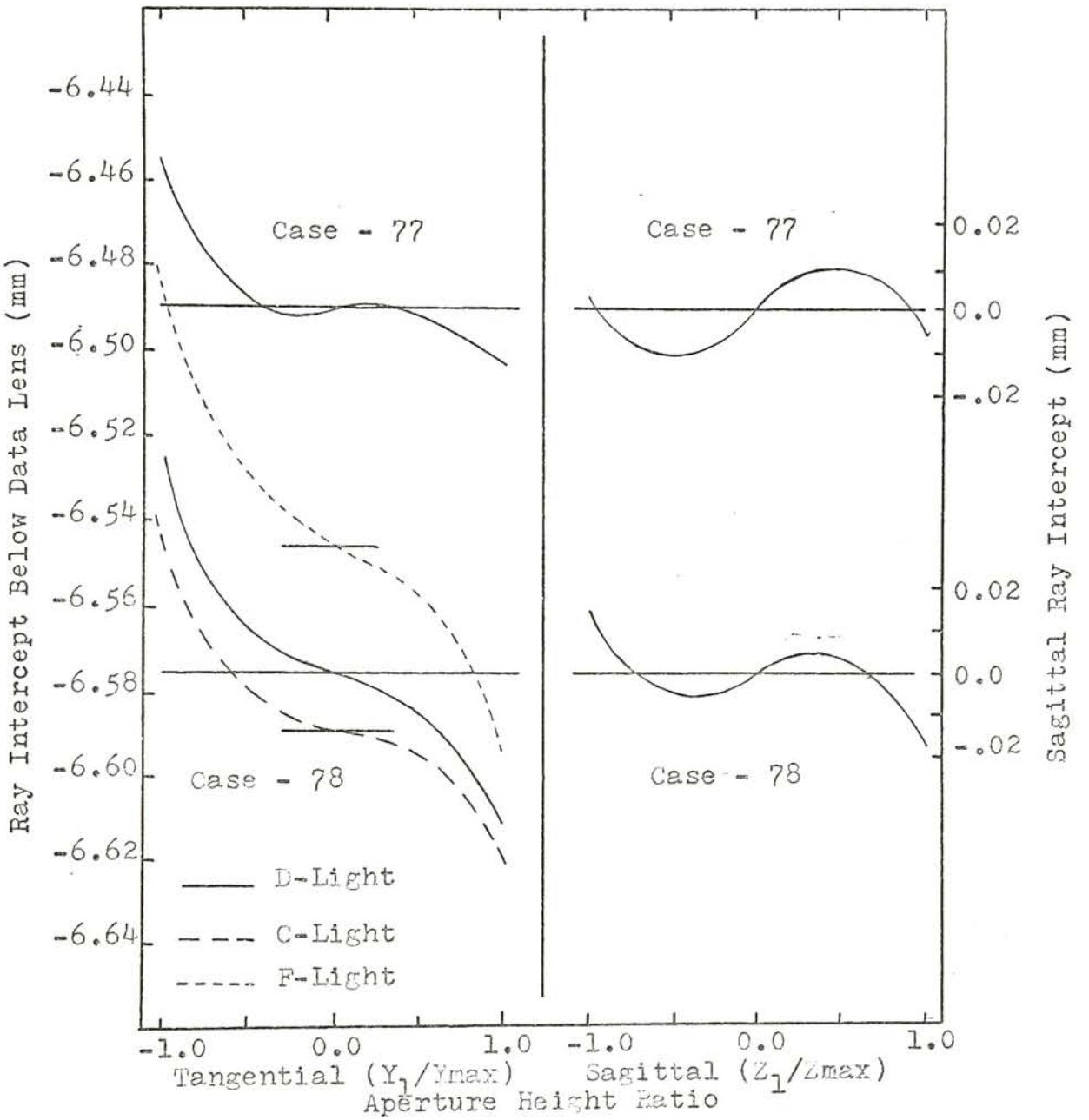

Figure A-6. Tangential and sagittal focus ray intercept curves.

Since the sharpness of the sagittal edges of the data image would most directly affect the aperture detection qualities of the system, the sagittal focus parameters of Case 78 were used in the final evaluations of image quality. A total of 49 rays, uniformly distributed over the system aperture, were traced through the data system to provide the spot diagram of Figure A-7. The edge and radial energy distributions shown in Figure A-8 were obtained by appropriately scanning the spot diagram. A combined modulation transfer function for the sagittal and tangential effects can be obtained by using the radial energy distribution of Figure A-8. The resulting modulation transfer for this data system design is presented in Figure A-9 and is, no doubt, degraded by the poor tangential quality of the image. For a compromise focus, improvement of the modulation transfer is to be expected.

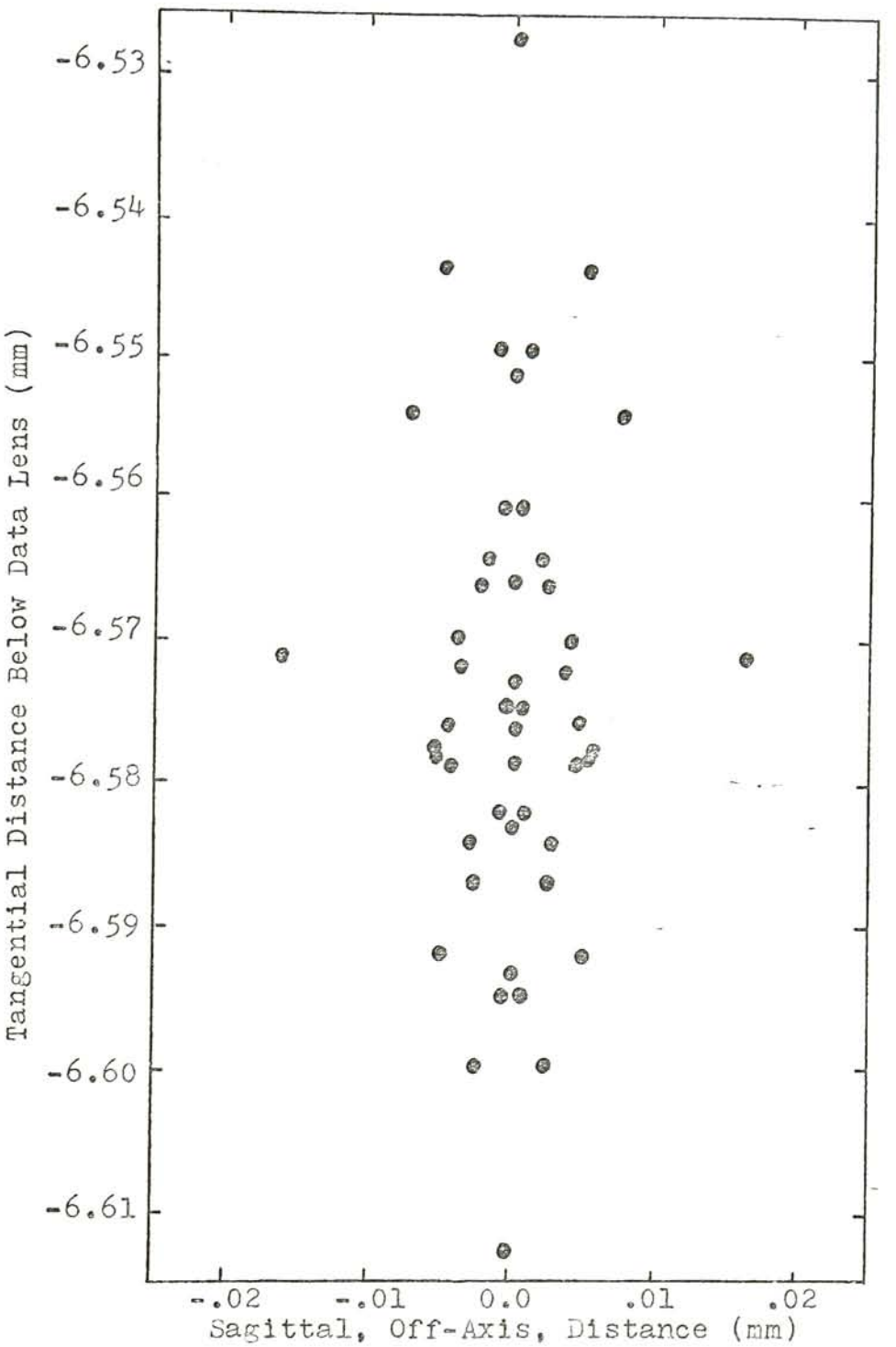

Figure A-7. Spot diagram for sagittal focus, Case 78.

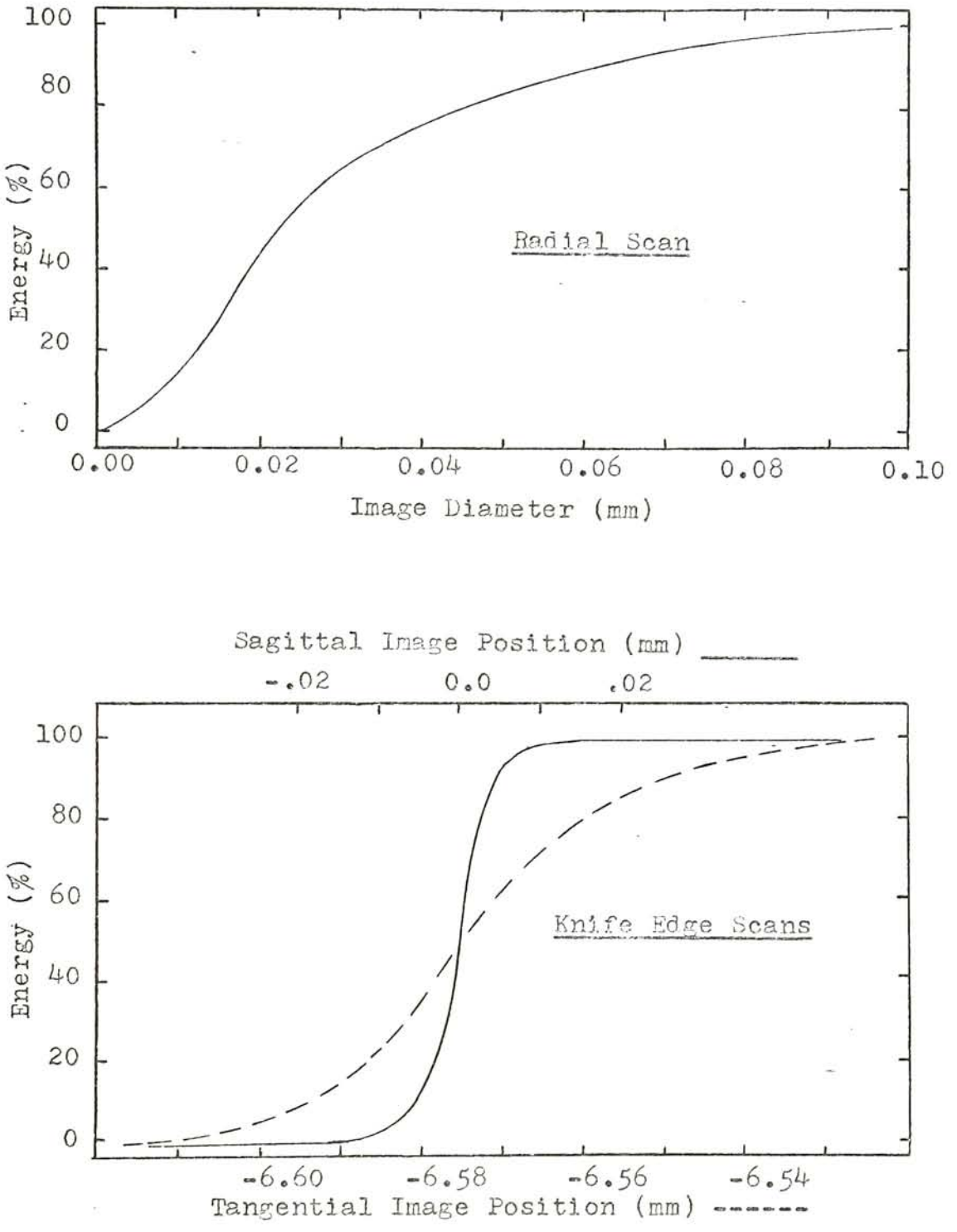

Figure A-8. Image energy distributions, sagittal focus.

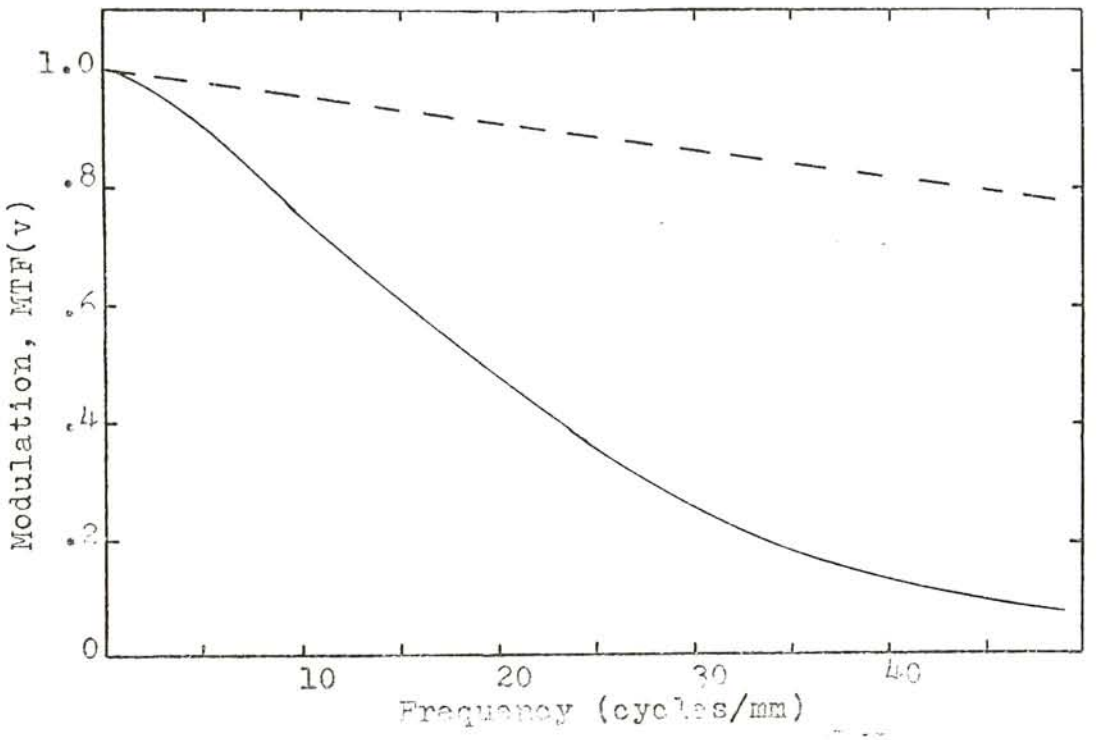

- - - - - Diffraction Limit

——— Radial MTF determined from radial energy distribution with approximation equation:[6]

$$MTF(v) = \sum_{i=1}^{m} \Delta E_i \, J_o(2\pi v \bar{R}_i)$$

where v is the frequency

ΔE_i is the energy difference for i-th radial strip

$\bar{R}_i$ is the average radius of the i-th strip

$J_o( )$ is zero order Bessel Function

Figure A-9. Radial modulation transfer for sagittal focus.

APPENDIX B

Statistics of Calibration

Preliminary experimental results indicated that the functional relationships between the image parameters and the camera settings were quadratic in nature. For this reason, five settings for focus and for aperture were selected as calibration levels, viz, f/5.6, f/8, f/9.5, f/11, and f/16; 3, 5(detented), 8, 15(detented), 70(detented), and infinity. These levels were crossed fully to produce twenty-five exposure combinations which were used in random order within each of six replications for each film type. In all, 300 calibration exposures were made and only one-third of these were measured eventually.

The position and width measurements for the images were made in accordance with the technique described in Figure 7. Two measurements of each parameter of each image were obtained producing a total of 200 pairs of measurements. Therefore, each exposure combination was represented by eight measurement pairs, four for position and four for width. When measurements are made in this manner, the simple average of the measurements in an exposure combination has meaning, but the simple standard deviation does not. The measurements are, in fact, nested within their image and the images are themselves independent replicates of the particular exposure combination.[15]

When the measurements for position and for width were collected into groups of similar aperture value, obvious changes in variation occurred between all of the width groups and all of the position groups except those of f/5.6 and f/8. The position measurements for these two groups were the same basically, thereby, reflecting their similar

origin-vignetted images. Each grouping of data then could be represented as a three factor, nested experiment as follows

Factor A = Exposure combinations for same aperture (or physical cause), 5 (or 10) levels

Factor B = Images for each exposure combination, 4 levels

Factor C = Measurements for each image, 2 levels

In this way, the calibration measurements were divided into eight groupings of 40 data points each and one group of 80 points.

A separate analysis of variance (ANOVA) was performed on each of the nine measurement groupings using the ANOVA program available in the Institute's Computer Center. The only required adjustment of the computed results was the combining of the interactions with their main effects because of the nested property of the data. The degrees of freedom and estimated mean squares (EMS) for these ANOVA results are shown in Table B-1.

Table B-1. Degrees of freedom and EMS terms for ANOVA

SOURCE	DEGREES OF FREEDOM	EMS
A (between combinations)	4 (9)	$8\sigma_A^2 + 2\sigma_B^2 + \sigma_C^2$
B (between images)	15 (30)	$2\sigma_B^2 + \sigma_C^2$
C (between measurements)	20 (40)	σ_C^2

The degrees of freedom in parentheses are for the f/5.6 and f/8 position ANOVA. Variance estimates were made for all the sources of variability and the computed 95% confidence limits are listed in Table 3.

From the EMS considerations, it is clear that the variance between measurements can be determined uniquely and, as stated in the text, these values for all nine groupings were not significantly different. By pooling the measurement variances from the groups, the total measurement variance with 200 degrees of freedom was obtained. In contrast, the variances from the changes between images of the same exposure combination could not be determined exactly; only the B-to-C variance ratios could be found with statistical rigor. These variance ratios were cleared, however, by using the computed measurement variances for each group. This action seemed justified by the fact that relatively large degrees of freedom had been used in the determination of the measurement variance and the variance ratios.[16]

The variation in data image width can be related to the variation in the camera iris through use of the data system magnification. Let s represent the maximum variation in average image width, w, for a particular aperture setting, then the total possible change in image width is

$$\Delta_w = (w + s) - (w - s) = 2s$$

Since the image area is proportional to the square of the width, the total possible change in image area is

$$\Delta_A = K(w + s)^2 - K(w - s)^2 = 4Kws$$

where K is a proportionality constant. Now the average image area, A, is

$$A = Kw^2$$

and the percentage change in image area becomes

$$\% \text{ Image Area Change} = \frac{4Kws(100)}{Kw^2} = 4\frac{s}{w}(100)$$

The magnification of the data system, M_1, can be found by comparing the average image width at f/5.6 with the design width of the iris.[11]

$$M_1 = \frac{\text{image width}}{\text{iris width}} = \frac{4.47}{11.01} = 0.41$$

The percentage change in iris area becomes

$$\% \text{ Iris Area Change} = (98.0)\frac{S}{W}$$

and the percentage iris width change is

$$\% \text{ Iris Width Change} = (49.0)\frac{S}{W}$$

The computed iris changes for s equal to the upper 95% confidence limit are provided in Table 4.

The average position measurements for each exposure combination were grouped according to aperture and the functional relationship between position and camera focus for each group determined by polynomial regression using the POLRG program of the Computer Center. To eliminate any program difficulties resulting from the infinity focus setting, the values of camera lens position change from the 3-feet setting, Table A-1, were used instead of the actual focus settings. These coded focus values provide the added convenience of simplified plotting and are quite useful in the formulation and evaluation of the computer program described in Appendix C.

The quadratic regression results for position versus focus were the most realistic and are graphically shown in Figure 8 and algebraically presented as follows:

(B-1) $P(\text{vignetted}) = -0.00292F^2 + 0.22185F + 2.21770$

(B-2) $P(f/9.5) = -0.00262F^2 + 0.19386F + 2.35513$

(B-3) $P(f/11) = -0.00198F^2 + 0.19467F + 2.54006$

(B-4) $P(f/16) = -0.00327F^2 + 0.20848F + 2.81622$

Where P is the image position and F is the coded focus value. The residual differences between the measured and the calculated

position values are shown in Table B-2.

Table B-2. Position estimate residuals (mm)

Focus(ft.)	Vignetted	f/9.5	f/11	f/16
3	0.0007	0.0013	0.0011	0.0003
5(det.)	-0.0038	-0.0064	-0.0035	-0.0014
8	0.0033	0.0047	-0.0035	0.0010
15(det.)	0.0011	0.0034	0.0110	0.0007
Infinity	-0.0013	-0.0029	-0.0051	-0.0006

The residuals are small and represent a total mean square error about regression of only 0.000034 with 19 degrees of freedom.[17] Comparison of a and k in Table 3 reveals that the positional regression error is only slightly larger than that for measurement alone.

Likewise, the average width measurements were grouped according to focus setting and the functional relationships between image width and camera aperture were found by polynomial regression. In these cases, the aperture values were coded by their stop relationships, i.e., f/5.6 = 1.00, f/8 = 2.00, f/9.5 = 2.50, etc. Stronger quadratic relationships between width and aperture were found as shown in Figure 9 and below

(B-5) $W(3) = 0.11434A^2 - 1.40502A + 5.49031$

(B-6) $W(5d) = 0.11221A^2 - 1.42749A + 5.72515$

(B-7) $W(8) = 0.10677A^2 - 1.41931A + 5.81973$

(B-8) $W(15d) = 0.11884A^2 - 1.49156A + 5.95563$

(B-9) $W(INF) = 0.10851A^2 - 1.44968A + 5.99712$

where W is the image width and A is the coded aperture value. The corresponding residuals are shown in Table B-3.

Table B-3. Width estimate residuals (mm)

Aperture	3	5d	8	15d	INF
f/5.6	-0.0021	0.0022	-0.0017	-0.0000	0.0055
f/8	0.0075	-0.0076	0.0072	-0.0057	-0.0286
f/9.5	-0.0030	0.0024	-0.0056	0.0154	0.0320
f/11	-0.0041	0.0049	-0.0009	-0.0116	-0.0073
f/16	0.0018	-0.0019	0.0010	0.0019	-0.0016

These residuals represent a total mean square error about regression of 0.000128 with 24 degrees of freedom. This larger regression error is to be expected because of the larger variability of the width data, cf., 1 with f through j of Table 3.

APPENDIX C

Aperture and Focus Calculation Method

Neither the curves of Figures 8 and 9 nor the regression equations of Appendix B offer straightforward means of determining the camera settings from a pair of image measurements. An accurate and efficient method of calculation is required if the data system is to be of any practical use. The interdependence of the regression equations upon aperture and focus requires that both position and width be used in the determination of the settings. This interdependence, in fact, makes possible the iterative computational method described in this appendix.

Examination of the regression equations of Appendix B reveals that when an aperture value is assumed, the position vs. focus equation is specified and vice-versa. A Fortran IV computer program based upon this interdependence was written and successfully used. A flow-chart of the primary computer operations is supplied in Figure C-1. In summary, the image width measurement is compared with the maximum width limits for each aperture value as found during system calibration. The first aperture estimation is obtained from this comparison and is used to select a position vs. focus equation. The position measurement then is used in the equation to determine the first focus value. This focus value then specifies a width vs. aperture equation which is used along with the original width measurement to determine an improved aperture value. The calculation cycle is repeated until there is a sufficiently small change in the estimated focus value. The final focus and aperture results are printed out as the "Best..." values. The program then places 95% confidence limits on these best

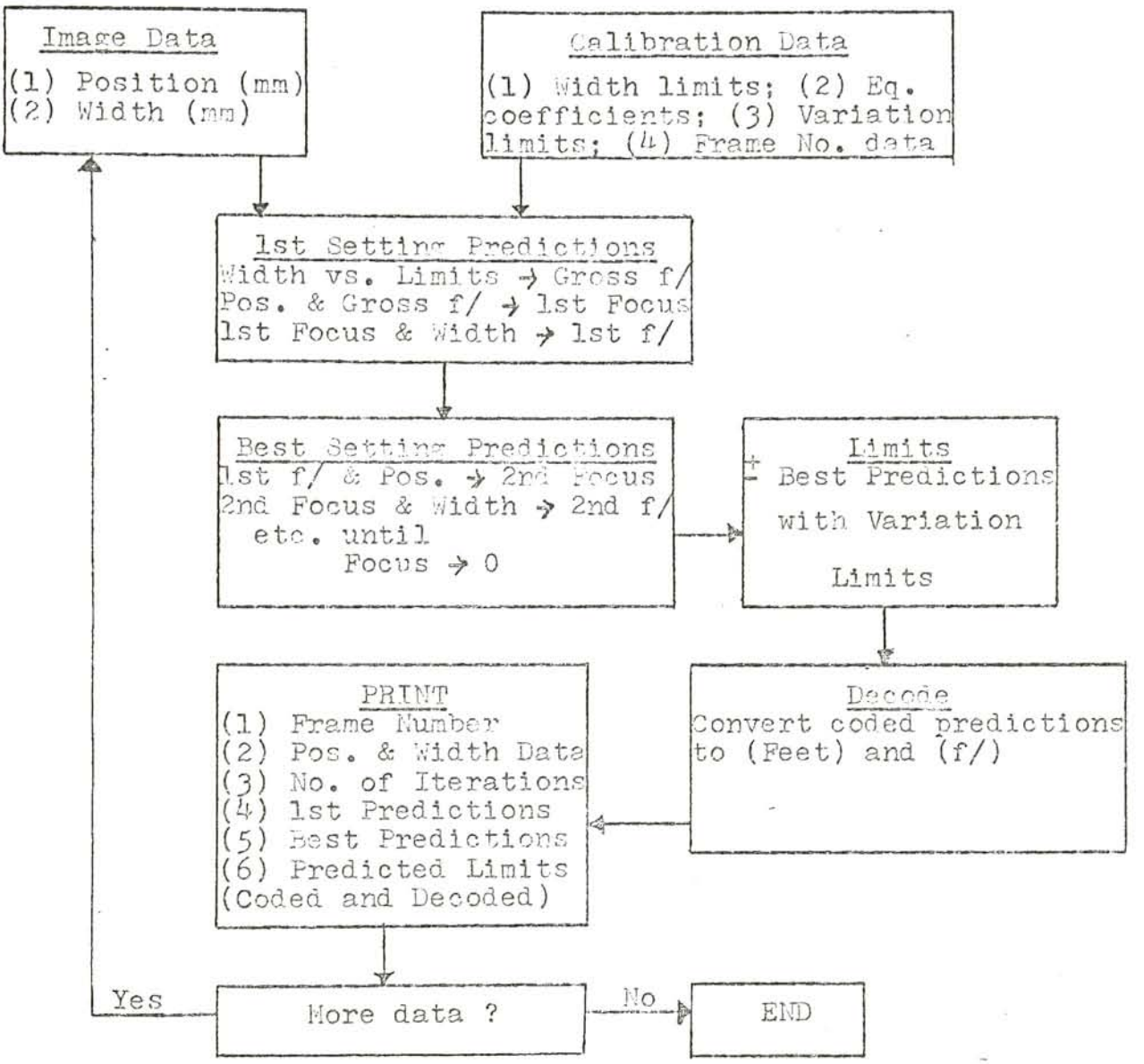

Figure C-1. Predictive program flow-chart.

values by including both the measurement and the program regression errors. Separate focus and aperture error quantities are permitted and a typical data output format is shown in Table C-1.

Table C-1. Predictive program output format

FRAME NUMBER = 52		WIDTH = 3.066000
POSITION = 3.062000		NO. OF ITERATIONS = 4
2.436	9.306	FIRST APERTURE EST. (CODED, F/=)
2.447	9.341	*BEST APERTURE ESTIMATE*
2.497	9.506	MIN-APERTURE ESTIMATE
2.397	9.181	MAX-APERTURE ESTIMATE
3.845	21.317	FIRST FOCUS EST. (CODED, FEET)
3.964	26.686	*BEST FOCUS ESTIMATE*
3.835	20.946	MIN-FOCUS ESTIMATE
4.094	36.874	MAX-FOCUS ESTIMATE

The program, for the most part, uses approximations of the exact regression equations and the nature of these approximations must be understood. The single position vs. focus equation for vignetted apertures, equation (B-1), applies for settings of f/5.6 through f/8 and is used in its exact form. The position relationships for the remaining aperture values have a similar physical origin and, therefore, are approximated by a single relationship. The main coefficients for this approximated position relation are themselves functions of aperture as determined by regression of the appropriate coefficients of equations B-2 through B-4. The positional relationship for the non-vignetted settings then becomes

(C-1) $P = C_7F^2 + C_8F + C_9$

where

$$C_7 = -0.00262$$
$$C_8 = 0.00813A^2 - 0.04313A + 0.25090$$
$$C_9 = -0.06260A^2 + 0.71433A + 0.96057$$

C_7 is the average of the quadratic coefficients of equations B-2 through B-4; C_8 is the regression result for the linear coefficients; C_9 is the regression result for the constant coefficients. In a similar manner, a single approximated width vs. aperture relationship is obtained from equations B-5 through B-9 as follows

(C-2) $$W = C_{13}A^2 + C_{14}A + C_{15}$$

where

$$C_{13} = 0.112134$$
$$C_{14} = -0.00011F^2 - 0.01358F - 1.40265$$
$$C_{15} = 0.11874F + 5.49237$$

The only way to measure how well the equation approximations represent the original regression results is to use the calibration regression data in the program and determine the resulting residuals. A slight modification to the program permits this check and furnishes the desired residuals automatically. The program position and width residuals are presented in Tables C-2 and C-3 respectively.

Table C-2. Program position residuals

Focus(ft)	Vignetted	f/9.5	f/11	f/16
3	0.0007	0.0021	0.0035	0.0098
5d	-0.0038	-0.0027	0.0034	-0.0005
8	0.0033	0.0067	0.0048	-0.0052
15d	0.0011	0.0014	0.0039	-0.0107
INF	-0.0014	0.0067	0.0000	-0.0206

Comparison with Tables B-2 and B-3 indicates that the general magnitudes of the program residuals are a little higher than for the initial regressions. Furthermore, the program residuals are no longer evenly distributed about each setting and the residual sums for position and for width are 0.0022 and -0.0072 respectively.

Table C-3. Program width residuals

Aperture	3	5d	8	15d	INF
f/5.6	-0.0047	0.0048	0.0039	0.0033	-0.0036
f/8	0.0093	-0.0026	0.0198	-0.0207	-0.0334
f/9.5	0.0019	0.0083	0.0047	-0.0040	0.0228
f/11	0.0052	0.0097	0.0072	-0.0328	-0.0155
f/16	0.0225	0.0073	-0.0019	-0.0058	-0.0130

The mean squares about "regression" of 0.000069 for position and 0.000228 for width more precisely specify the error increases from use of the program. However, when these mean squares are compared with the exact ones of Appendix B, no significant difference exists for a 95% confidence level. Furthermore, without use of the program, the errors from interpolation and graphical approximation certainly would be even larger. It is also possible that the program results could be enhanced by the suggested calibration procedures because better initial data fits could be obtained and the important position vs. focus relation for f/13.2 would then exist.

APPENDIX D

Statistics of Field Test

The basic characteristics of the system field tests, described in section III. D, are summarized as follows:

(a) The seven half-stop aperture settings from f/5.6 through f/16 were used in random sequence.

(b) The marked and the detented focus settings of 3, 3.5, 4, 5d, 6, 8, 10, 15d, 30, 70d, and infinity were used in random sequence, independently of the aperture settings.

(c) More than one-hundred exposures on each film type were obtained of scenes on the R.I.T. campus. Full daylight and the resulting shadows were used for scene illumination. From these exposures, one-hundred black and white and twenty-five color data images were measured and evaluated as described in section IV. B.

When the recorded focus values were compared with the results from the computer program, a significant bias to low values was found. Figure D-1 conveniently portrays this bias in frequency histogram form for both the individual focus values and the cumulative total. The individual histograms suffer from an insufficiency of points, but do indicate the consistent bias. The total focus histogram further substantiates the bias and also shows bimodal tendencies which would indicate the possibility of two causes for the bias. The accentuated spread to the right of the infinity focus histogram led to a realization that the independent randomization of the aperture and focus settings was not a good way to produce well-distributed exposure situations, because more than half of the infinity focus exposures measured were taken at f/16. Complete

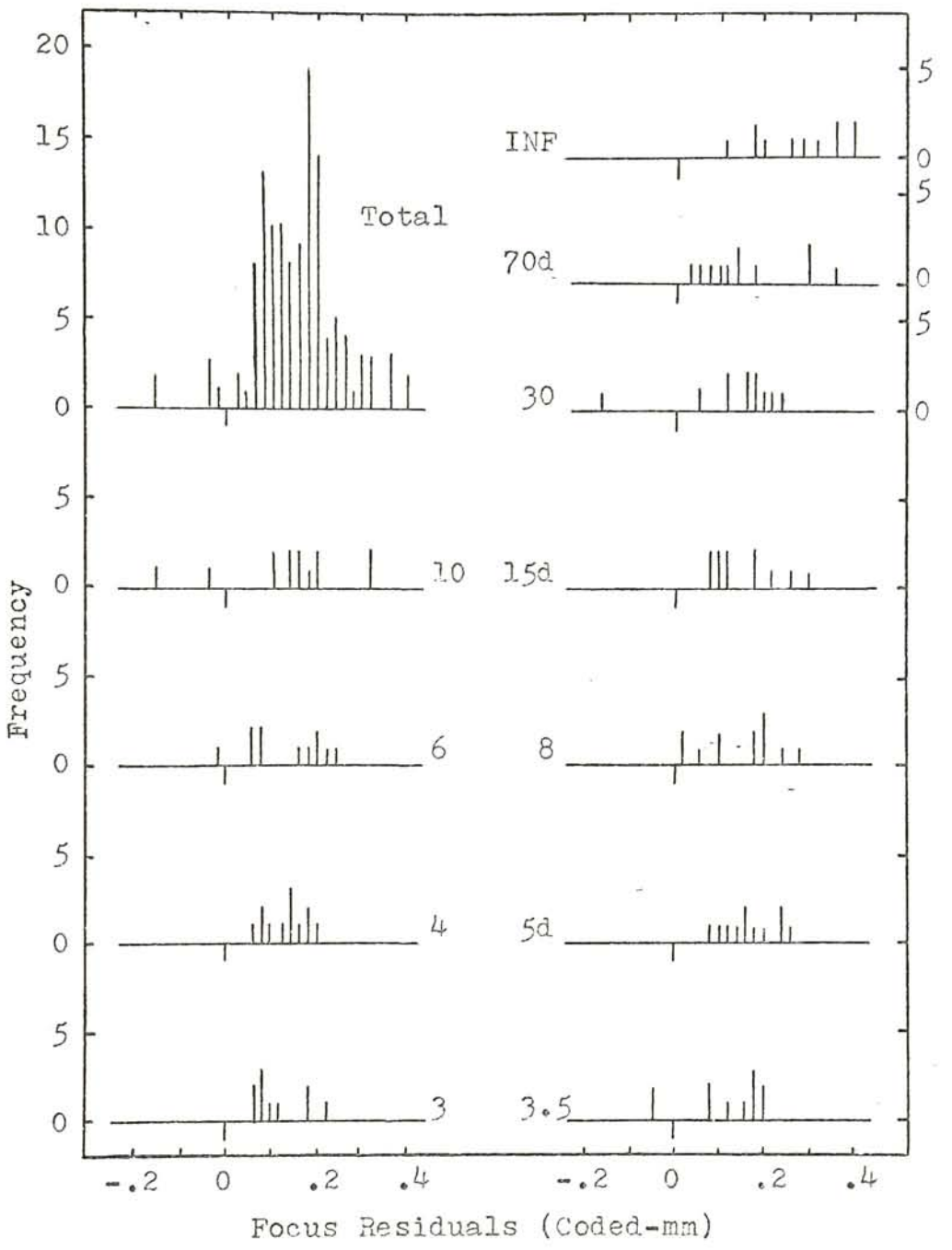

Figure D-1. Field test focus residuals.

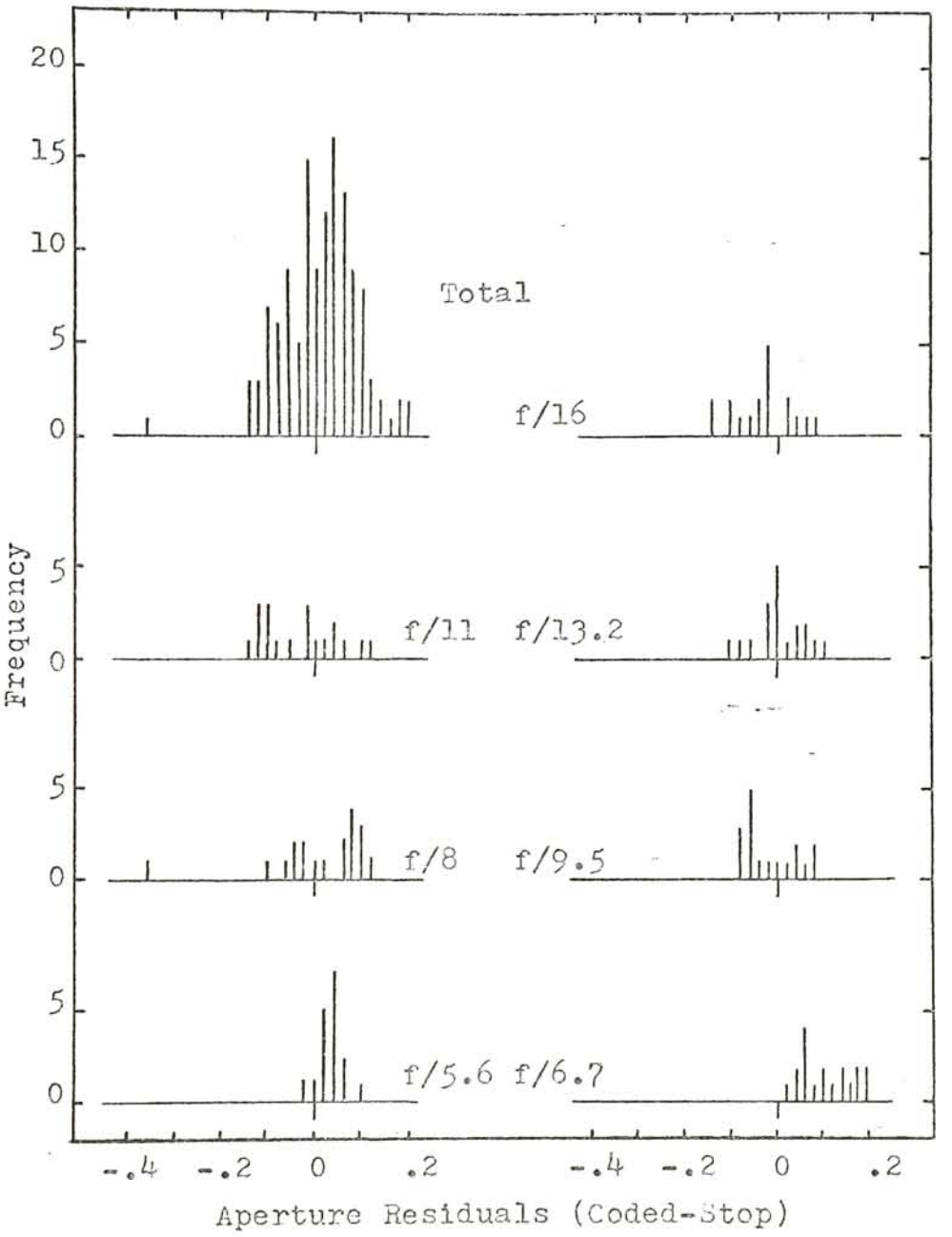

Figure D-2. Field test aperture residuals.

crossing of the settings would have required only 77 exposures and would have provided an even mixture of combinations.

Figure D-2 shows the same histogram type presentation for the field test aperture residuals. The total frequency plot exhibits a good normal shape and has only a slight bias to the lower values. The one flyer data point to the far left represents black and white frame number 59 in which the data image was almost completely obscured in shadow. The individual histograms are well centered about the zero except for those of f/6.7 and f/5.6. These two contributions appear to be the cause of the small total bias and probably result from an inadequacy in the regression relationships. An inclusion of the f/6.7 setting in the system calibration would improve this situation.